Small Science

Robust Synthesis of Targeting Glyco-nanoparticles for Surface Enhanced Resonance Raman Based Image-Guided Tumor Surgery --Manuscript Draft--

Manuscript Number:	smsc.202300154R1
Article Type:	Research Article
Corresponding Author:	Xuefei Huang, Prof. Michigan State University East Lansing, Michigan UNITED STATES
Corresponding Author E-Mail:	huangxu2@msu.edu
Order of Authors (with Contributor Roles):	Kunli Liu, PhD (Data curation: Lead; Investigation: Equal; Methodology: Equal; Writing – original draft: Equal; Writing – review & editing: Supporting)
	AKM Atique Ullah (Data curation: Supporting; Investigation: Equal; Methodology: Equal; Writing – review & editing: Equal)
	Aniwat Juhong (Data curation: Supporting; Investigation: Supporting)
	Chia-wei Yang (Data curation: Supporting)
	Cheng-you Yao, PhD (Data curation: Supporting)
	Xiaoyan Li, PhD (Data curation: Supporting)
	Harvey Bumpers, MD (Data curation: Supporting; Writing – review & editing: Supporting)
	Zhen Qiu, PhD (Conceptualization: Equal; Funding acquisition: Equal; Supervision: Equal)
	Xuefei Huang, Prof. (Conceptualization: Equal; Funding acquisition: Equal; Supervision: Lead; Writing – original draft: Equal; Writing – review & editing: Lead)
Keywords:	glyco-nanoparticles; imaging guided surgery; Surface enhanced Raman spectroscopy; synthesis
Manuscript Classifications:	DIAGNOSIS & THERAPY - nanomedicine, drug delivery, pharmacology, therapeutics, diagnostics, theranostics, imaging, disease prevention
Section/Category:	
Abstract:	Surface Enhanced Resonance Raman (SERS) is a powerful optical technique, which can help enhance the sensitivity of Raman spectroscopy aided by noble metal nanoparticles (NPs). However, current SERS-NPs are often suboptimal, which can aggregate under physiological conditions with much reduced SERS enhancement. Herein, a robust one-pot method has been developed to synthesize SERS-NPs with more uniform core diameters of 50 nm, which is applicable to both non-resonant and resonant Raman dyes. The resulting SERS-NPs are colloidally stable and bright, enabling NP detection with low-femtomolar sensitivity. An algorithm has been established, which can accurately unmix multiple types of SERS-NPs enabling potential multiplex detection. Furthermore, a new liposome-based approach has been developed to install a targeting carbohydrate ligand, i.e., hyaluronan, onto the SERS-NPs bestowing significantly enhanced binding affinity to its biological receptor CD44 overexpressed on tumor cell surface. The liposomal HA-SERS-NPs enabled visualization of spontaneously developed breast cancer in mice in real time guiding complete surgical removal of the tumor, highlighting the translational potential of these new glyco-SERS-NPs.
Author Comments:	
Additional Information:	
Question	Response
Please submit a plain text version of your	Dear Dr. Rhode,

cover letter here.

We would like to submit a revised manuscript titled "Robust Synthesis of Targeting Glyco-nanoparticles for Surface Enhanced Resonance Raman Based Image-Guided Tumor Surgery". The manuscript ID is smsc.202300154. The two reviewers were positive about our original manuscript overall. At the same time, they have provided helpful suggestions. To address all the comments, we have carefully revised the manuscript and the supporting information. Two versions of the main text have been submitted. One has the major changes highlighted with a yellow background and with the track change turned on marking all changes. The second one is the clean copy with all changes accepted.

In the following, the major changes are detailed point-by-point.

Editorial comments:

1. We have noticed that some of the text in your manuscript overlaps with published works in the Methods section.

Response: We have revised the text to avoid the overlapping text.

2. Statistics: For original research, please check that your manuscript includes a subsection entitled "Statistical Analysis" at the end of the Experimental Section.

Response: A section on statistics has been added. Figure legends have been updated to include the statistical information where applicable.

Reviewer 1

1. General comments: This paper describes the preparation and biological evaluation of specific nanoparticles containing Raman type dyes for Surface-Enhanced Raman Scattering (SERS) tumor imaging and guided surgery. The authors have worked out methods for attaching a targeting agent (Hyaluronic acid) to the particles through a liposome-based formulation. The paper is well written, although there are areas of English syntax and usage that should be carefully proofed and addressed before publication. I think this journal is an appropriate vehicle for this work, although I do feel the novelty of the research and results is only moderate, at best. Gold nanoparticles (AuNPs) have a long history as a platform for enhancement of Raman dyes (SERS), and the primary advance here is the use of a liposome to allow attachment of enough HA molecules to be effective in tumor targeting. While I think the work is solid and material is well characterized, there are several questions to be answered before publication:

Response: We would like to thank the reviewer for the positive overall evaluation. We agree the concept of AuNPs and Au-SERS NPs are not new. The main advances we made in this work are the development of the liposomal SERS NP system, which led to significantly enhanced bindings with the biological target CD44. Furthermore, there are significant advantages in using a polysaccharide such as HA as the targeting agent.

Comment 1: 1)There are several areas in the paper where more citations are necessary. As mentioned, there is a long history of AuNPs/SERS dyes conjugates, and review go back more than a decade ago (one example: Shuming Nie, Chem. Soc. Rev. 2008, 37, 912-920). The end of the second paragraph of the paper states "Methods......are under development". There could be many references here as well as for the seed method of growing AuNPs which is well known. Check for other sentences as well. In addition, the seed method for creating AuNPs above 17 nm is also a well-known procedure, as is the problems with generating uniform particles

above 20-30 nm by the citrate method alone. References should be added, and the "novelty" of this synthetic protocol should be downplayed since it is known. Response: We thank the reviewer for pointing this out. We have added the references suggested as well as other pertinent references in this area. For example, please see Refs 4, 11-13, 22.

[4]X. M. Qian, S. M. Nie, Chem. Soc. Rev. 2008, 37, 912.
[11]F. Meikun, F. S. A. Gustavo, G. B. Alexandre, Anal. Chim. Acta 2020, 1097, 1.
[12]S. E. J. Bell, G. Charron, E. Cortés, J. Kneipp, M. L. de la Chapelle, J. Langer, M. Procházka, V. Tran, S. Schlücker, Angew. Chem. Int. Ed. 2020, 59, 5454.
[13]L. A. Lane, X. Qian, S. Nie, Chem. Rev. 2015, 115, 10489.
[22]J. Dong, P. L. Carpinone, G. Pyrgiotakis, P. Demokritou, B. M. Moudgil, KONA Powder Part. J. 2020, 37, 224.

2. Comment 2: The section entitled "Biocompatibility of SERS-NPs" is incorrectly labeled. Performing cytotoxicity studies is NOT biocompatibility; this pertains to the stability of particles in a biological milieu, such as blood or serum. Please perform these studies (stability in high salt, serum pH etc....) and report the results by UV/Vis or DLS. Also, the zeta potential of the particles needs to be measured for full characterization data.

Response: Following reviewer's suggestion, we have performed stability analysis as well as zeta potential measurements under a variety of conditions including changes in salt concentrations and the presence of serum proteins. UV/Vis, DLS, and zeta potential of the particles have been added. The results are presented in Figures S6 and Table S1.

Table S1. ζ potential measurements (mean \pm standard deviation, N =3). SamplesZeta Potential (mV) Au NP Seed -41 \pm 2 S420 SERS-NPs-36 \pm 2 S481 SERS-NPs-35 \pm 3 PEG-S420 SERS-NPs-22 \pm 1 HA-S481 SERS-NPs-28 \pm 2 Liposome-S420 SERS-PEG-13 \pm 4

Figure S6. Analysis of particle stability. a) Relative absorbance and b) hydrodynamic diameter of the liposome-S421 SERS-HA particle in water, PBS 1x, PBS 10x, without serum (-serum), and with serum (+ serum). No statistically significant changes in the relative absorbance data or the hydrodynamic diameters suggested the stability of the NPs in PBS and serum. SERS signal intensities of liposome-S421 SERS-HA stored at c) 4 °C or d) room temperature over time. For each column, the mean value with the standard deviation was plotted. For each concentration, the values were from three samples. No statistically significant change in SERS intensity was observed for the NPs stored at 4°C up to 3 weeks. NPs stored at room temperature showed some changes in SERS intensities only at the 3-week mark. Statistical analysis was performed using a two-way ANOVA. ns: P > 0.05. *: P

nanoparticles is very curious. There are a host of studies where Raman dyes were coated on AuNPs followed by coating with silica to stabilize the dyes on the metal surface. It is curious why this method did not work here since the methods here are not

Liposome-S481 SERS-HA-24 ± 3

different from other studies??

Response: The silica coating of AnNPs was successful in our hand. However, we observed significantly reduced SERS intensities following the coating. The decrease in SERS signal intensities following silica coating has been reported by others (Refs # 9; 49) While the exact reason for the decrease is not known, it is likely due to the displacement of SERS dye from NP surface due to silica coating.

[9]N. D. Israelsen, C. Hanson, E. Vargis, Sci. World J. 2015, 2015, 124582 and references cited therein

[49]Y. Zhang, X. Li, B. Xue, X. Kong, X. Liu, L. Tu, Y. Chang, Sci. Rep. 2015, 5, 14934.

4. Comment 4: The authors make the point that a reason to use HA is due to the expense and stability of monoclonal antibodies. While it is true that commercially available mAb are expensive, they can also be prepared recombinantly for lower prices. In addition, their long-term stability is rather good, as many of them are, as is well known, used clinically with great success in tumor therapy. Thus, I feel this "drawback" of mAbs should be toned down slightly. I agree that using an inexpensive polysaccharide is a worthy substitute, however, CD44 is also expressed on many normal cells (including stem cells) and is important in many cell adhesion and wound healing processes. A control with binding to normal cells expressing CD44 in the process of tumor therapy would be a useful comparison.

Response: We have toned down the discussion on drawback of mAbs. The reviewer is right that CD44 is also found on normal cells. CD44 is known to exist in three forms, the low affinity form, the inflammation-induced high affinity form, and the constitutively high affinity form. In normal cells, CD44 primarily exists in the low affinity form only with weak affinities toward HA binding. In contrast, CD44 is found to be in its constitutively highly affinity form on tumor cells. This discussion has been added to the manuscript as the following.

While antibodies can bestow high specificity in target binding, they can be expensive especially for pre-clinical studies (hundreds of \$ per 100 µg) and can denature upon extended storage. Although the cost of monoclonal antibodies can be potentially managed with wide clinical adaption, as an alternative, we explored polysaccharides such as HA[34] as the targeting ligand. HA is readily available commercially (~\$200/g), can be stored for extended periods, and is biocompatible as highlighted by its common usage in the cosmetic industry. A major receptor of HA in human bodies is the glycoprotein CD44.[35] On normal cells, CD44 exists primarily in the inactive low affinity form exhibiting minimal binding with HA,[36] which can be converted to the active high HA affinity structure in the presence of inflammatory signals.[37] In contrast, tumor-derived cells often express CD44 in its high-affinity state capable of constitutively binding HA,[38] and the high affinity CD44 is found over-expressed on the surfaces of a wide range of cancer cells.[39-41]

5)Comment 5: It is also curious that the HA NPs stick to the surface of the liposomes in that formulation and are so much better at binding CD44. One would think that the interaction between lipid and HA may hinder that interaction. And the fact that the thiolated HA did not result in much addition of HA to the AuNP-SERS surface is also curious, as many polysaccharides that bind to AuNP surfaces tend to stabilize these constructs by "wrapping" around the gold surface with the sugar polymer making them more biocompatible. I think more explanation about the results of the synthesis are warranted.

Response: We thank the reviewer for the question. It is interesting that the liposomal formulation of HA SERS-NP gave significantly stronger binding to CD44. HA is known

to interact with phospholipid as well besides the SERS-NP. It is possible that with the liposomal formulation, more HA can be attached leading to enhanced avidity with CD44.

It is known that HA can interact with phospholipids through hydrogen bonding and hydrophobic interactions with HA distributed in punctate patterns on lipid bilayer surface.[58-59]

6)Comment 6: When the issue of the various "flavors" of resonant, and non-resonant dyes comes up, I strongly feel that the structures should be in the main text of the manuscript, not in the SI. The author needs to see the structures that the authors are working with while reading the results section. They can, of course, remain in the SI, but they also need to be in the main text. And importantly, why did the authors use both bipyridyl and a fully deuterated analogue? Is this standard practice in SERS work? If it is, please add a sentence or two as to why these two are compared (for the uninitiated). I understand that H-D exchange can be detected by SERS, but why it is used here is unclear.

Response: We thank the reviewer for this suggestion. The structures of the dyes have been added to the main text as figure 1f.

The reason S420 and S421 (deuterium containing version of S420) are used is because they have distinctive Raman peaks (Figure 2a) helping to increase the number of dyes can be used. The following explanation has been added to the text.

Despite similarity in structures of some Raman dyes (for example S420 vs S421), these dyes have distinct fingerprint patterns in their respective Raman spectra potentially enabling multiplexing (Figure 2a).

7)Comment 7: There is a distinct lack of controls in the tumor work. While I understand that the authors are using the liposome-SERS-Peg particles as "non-targeting" controls, they also need to employ another tumor line which is known to not express CD44 as well as a normal line. There are other molecules that HA may bind to and this needs to be done side-by-side with tumor such as 4T1. The experimental section describing the guided imaging has no description of how in the Polyoma Middle-T antigen MMTV mice were generated: Were they purchased? Obtained as a gij? Also, that section states "A MUC1/MMTV mouse...." What is a MUC1/MMTV mouse? Are there mutant mucins involved such as MUC1? There needs to be a much more detailed description of this model and an explanation of why there is a "MUC1" in the description?

This is a nice paper, but some issues need to be resolved before publication. Response: We thank the reviewer for the suggestions. It is true that there are other receptors such as HA receptor for endocytosis (HARE), lymphatic vessel endothelial hyaluronan receptor 1 (LYVE-1) for HA besides CD44. However, these receptors are typically not found at tumor site as HARE is mainly expressed in liver and LYVE-1 is mainly found in lymphatic vessels. For the application of HA NPs in image guided surgery, they should not post much interference.

As the NPs are targeting CD44 overexpressed on tumor cells, they are not suitable to detect CD44 negative tumor. We have added the discussion on this limitation in the main text as the following:

There are limitations to our study. While many breast cancer cells express CD44,[39, 73] due to tumor heterogeneity, it is possible that there are cancer cells with low or no expression of CD44, which will not be detected using our approach. For more comprehensive cancer detection, biomarkers beyond CD44 can be targeted. With the potential for multiplexing, the SERS-NP strategy can be applied for simultaneous detection of multiple biomarkers in one imaging session, which is a direction we will pursue.

We have added the source and more information on the Polyoma Middle-T antigen MMTV mice. We apologize for the mentioning of MUC1, which was a mistake and has been corrected.

MMTV-PyMT transgenic mice were purchased from the Jackson Laboratory. In a span of 4 months, the female mice showed the spontaneous onset of palpable breast cancer. The mice were housed at Michigan State University's Laboratory Animal Resources Facility. All activities and protocols related to the animal study received approval from the Institutional Animal Care and Used Committee (IACUC) at Michigan State University.

Reviewer 2

1.Comment 1: The authors have reported a fairly novel one-pot synthesis of a stable SERS-NP that is colloidally linked to hyaluronic acid (HA) which would then specifically target CD44, a marker that is prominent in many cancers and in T-lymphocytes of inflammatory cells. If this technology is feasible and is relatively non-toxic then, the field has developed one more tool in detecting tumor and perhaps tumor margins in a surgical and post-tumor resection setting.

Response: We thank the reviewer for the positive feedback.

2.Comment 2: We are not in the position to rigorously review the chemical synthesis and characterization of the liposome-based HA-SERS-NP. However, it would have been nice if we had seen more stability data through DLS measurements using the Zetasizer or through examination of the stability of the Raman spectra over time or both? Do electron microscopy studies show changes in aggregations with respect to time of initial synthesis or with respect to storage temperature?

Response: We thank the reviewer for the suggestions. We have performed additional stability studies. The additional results including DLS, zeta potential and stability over time are now presented in Table S1 and Figure S6. There were not significant changes in particle sizes with respect to time or storage temperature. Please see response to reviewer 1 comment 2.

3.Comment 3: I also have some questions as to how they conducted their toxicity and preclinical safety studies. I noticed that the MTS assay for in vitro cellular viability when challenged with the SERS-NP was on Raw 264.7 cells (Figure S4) (a macrophage cell line?). No toxicity was reported up to 100 pM. It would have been nice to see a fuller toxicity/dose response study where an actual LD50 number was obtained. Also aside from the MTS study, we do not see the Raw 264.7 cells again in the report. The authors focus primarily on 4T1 cells to study NP specificity (Figure 4) and I think they use the MUC1/MMTV mouse models to examine in vivo/preclinical uptake of surgical-guided SERS-NP-HA onto spontaneous tumors (Figure 5). Thus it is unclear, how generalizable across different cancer cell lines are the safety and specificity data they present on their SERS-NP. Indeed, it is not clear in their studies how specific are their NPs are to cancer cells as opposed to inflammatory cells. This will become important

even in their limited application of a post-resection setting as the tumor microenvironment often is populated with inflammatory immune cells. Response: We thank the reviewer for the questions. To be consistent, we have performed additional cell viability studies with 4T1 breast cancer cells (Figure S4). The particles did not significantly affect the cell viability up to 500 pM. Typical concentrations of the NP used for in vitro and in vivo experiments were below 250 pM. For the MTS viability assay, we were not able to get to higher NP concentrations as the NP is also colored and would interfere with the optical absorbance reading in MTS assay at higher NP concentrations.

Figure S4. MTS assays with 4T1 breast cancer cells indicated the NPs did not affect the cell viabilities under the experimental condition. 4T1 cells were incubated with a) liposome-S440 SERS-PEG or b) Liposome-S421 SERS-HA for 4 h under various NP concentrations: 0 pM, 10 pM, 20 pM, 50 pM, 100 pM, 200 pM, 300 pM, and 500 pM. No significant changes in cell viability were observed suggesting the NPs were not toxic to cells up to at least 500 pM. For each column, the mean value with the standard deviation was plotted. For each concentration, the values were from three samples. Statistical analysis was performed using a two-way ANOVA. ns: P > 0.05.

As discussed in responses to Reviewer 1's comment 7, CD44 on normal cells are typically in a low affinity state, with little binding to HA. Thus, the SERS-NP-HA can readily differentiate normal cells vs CD44 expressing tumor cells. Our NP probes selectively target CD44, which will not bind with CD44 negative tumor cells. This is a limitation of the current study, which has been discussed in the text as the following:

There are limitations to our study. While many breast cancer cells express CD44,[39, 73] due to tumor heterogeneity, it is possible that there are cancer cells with low or no expression of CD44, which will not be detected using our approach. For more comprehensive cancer detection, biomarkers beyond CD44 can be targeted. With the potential for multiplexing, the SERS-NP strategy can be applied for simultaneous detection of multiple biomarkers in one imaging session, which is a direction we will pursue.

The reviewer is right that some inflammatory cells can bind with CD44. In the tumor microenvironment, immune cells can infiltrate into tumor tissues and be mixed with cancer cells. Therefore, for complete elimination of tumor at the tumor site, it is common to surgically remove the infiltrated immune cells together with tumor. As the NPs are applied only locally to the tumor site in our application, only cells in the tumor site will be removed. Thus, the imperfect selectivity of tumor vs immune cells is not a significant drawback.

In summary, we are very grateful for reviewers' comments, which help us develop a stronger manuscript. With the revisions made, I hope the paper can now be accepted. If you would require any further information, please do not hesitate to contact us.

Sincerely,

Xuefei Huang, Ph. D.

Does the research described in this manuscript include animal experiments?

Yes

Please confirm that ethical approval from the national or local authorities was obtained prior to the research, and that this is included in the Experimental section of your manuscript. as follow-up to "Does the research described in this manuscript include animal experiments?"	Yes, I confirm
Please provide the name of the national or local authority giving the approval in the textbox below, as well as in the Experimental section of your manuscript. as follow-up to "Please confirm that ethical approval from the national or local authorities was obtained prior to the research, and that this is included in the Experimental section of your manuscript."	Michigan State University IACUC
If available, please provide the assigned approval/accreditation number of the laboratory/investigator in the textbox below, as well as in the Experimental section of your manuscript. as follow-up to "Please confirm that ethical approval from the national or local authorities was obtained prior to the research, and that this is included in the Experimental section of your manuscript."	PROTO202100095
Does the research described in this manuscript include human research participants (including for experiments with sensors or wearable technologies) or tissue samples from human subjects (including blood or sweat)?	No
Do you or any of your co-authors have a conflict of interest to declare?	No. The authors declare no conflict of interest.
Response to Reviewers:	Please see cover letter submitted.

MICHIGAN STATE UNIVERSITY

Nov. 14th, 2023

Dear Dr. Rhode,

We would like to submit a revised manuscript titled "Robust Synthesis of Targeting Glyco-nanoparticles for Surface Enhanced Resonance Raman Based Image-Guided Tumor Surgery". The manuscript ID is smsc.202300154. The two reviewers were positive about our original manuscript overall. At the same time, they have provided helpful suggestions. To address all the comments, we have carefully revised the manuscript and the supporting information. Two versions of the main text have been submitted. One has the major changes highlighted with a yellow background and with the track change turned on marking all changes. The second one is the clean copy with all changes accepted.

In the following, the major changes are detailed point-by-point.

Editorial comments:

1. We have noticed that some of the text in your manuscript overlaps with published works in the Methods section. In order to avoid any ethical issues, the overlapping parts should be re-worded to minimize any direct similarity to previous publications (of course author information, acknowledgements, and references can be ignored; to resolve significant overlap in the Experimental Section, methods can be abbreviated and the original source cited). Please contact the editorial office if you have any questions.

Response: We have revised the text to avoid the overlapping text.

2. Statistics: For original research, please check that your manuscript includes a sub-section entitled "Statistical Analysis" at the end of the Experimental Section that fully describes the following information: 1. Pre-processing of data (e.g., transformation, normalization, evaluation of outliers), 2. Data presentation (e.g., mean \pm SD), 3. Sample size (n) for each statistical analysis, 4. Statistical methods used to assess significant differences with sufficient details (e.g., name of the statistical test including one- or two-sided testing, testing level (i.e., alpha value, P value), if applicable post-hoc test or any alpha adjustment, validity of any assumptions made for the chosen test), 5. Software used for statistical analysis.

Figure legends: Please make sure that all relevant figure legends contain the information on sample size (n), probability (P) value, the specific statistical test for each experiment, data presentation and the meaning of the significance symbol.

Response: A section on statistics has been added. Figure legends have been updated to include the statistical information where applicable.

Reviewer 1

1. General comments: This paper describes the preparation and biological evaluation of specific nanoparticles containing Raman type dyes for Surface-Enhanced Raman Scattering (SERS) tumor imaging and guided surgery. The authors have worked out methods for attaching a targeting agent (Hyaluronic acid) to the particles through a liposome-based formulation. The paper is well written, although there are areas of English syntax and usage that should be carefully proofed and addressed before publication. I think this journal is an appropriate vehicle for this work, although I do feel the novelty of the research and results is only moderate, at best. Gold nanoparticles (AuNPs) have a long history as a platform for enhancement of Raman dyes (SERS), and the primary advance here is the use of a liposome to allow attachment of enough HA molecules to be effective in tumor targeting. While I think the work is solid and material is well characterized, there are several questions to be answered before publication:

Response: We would like to thank the reviewer for the positive overall evaluation. We agree the concept of AuNPs and Au-SERS NPs are not new. The main advances we made in this work are the development of the liposomal SERS NP system, which led to significantly enhanced bindings with the biological target CD44. Furthermore, there are significant advantages in using a polysaccharide such as HA as the targeting agent.

Comment 1: 1) There are several areas in the paper where more citations are necessary. As mentioned, there is a long history of AuNPs/SERS dyes conjugates, and review go back more than a decade ago (one example: Shuming Nie, Chem. Soc. Rev. 2008, 37, 912-920). The end of the second paragraph of the paper states "Methods.....are under development". There could be many references here as well as for the seed method of growing AuNPs which is well known. Check for other sentences as well. In addition, the seed method for creating AuNPs above 17 nm is also a well-known procedure, as is the problems with generating uniform above 20-30 bv the citrate method alone particles nm (see for example https://urldefense.com/v3/ https://doi.org/10.14356/kona.2020011 ;!!HXCxUKc!y9j1ZJSTx9evSmxpU3e-N xdD-CzRNO2TlrSr21i5x6WZY67i0nRnAaVj4eUfEEpxB2pfRurPUHKRx94cQ\$). References should be added, and the "novelty" of this synthetic protocol should be downplayed since it is known.

Response: We thank the reviewer for pointing this out. We have added the references suggested as well as other pertinent references in this area. For example, please see Refs 4, 11-13, 22.

```
[4] X. M. Qian, S. M. Nie, Chem. Soc. Rev. 2008, 37, 912.
```

[11] F. Meikun, F. S. A. Gustavo, G. B. Alexandre, *Anal. Chim. Acta* **2020**, *1097*, 1.

[12] S. E. J. Bell, G. Charron, E. Cortés, J. Kneipp, M. L. de la Chapelle, J. Langer, M. Procházka, V. Tran, S. Schlücker, *Angew. Chem. Int. Ed.* **2020**, *59*, 5454.

[13] L. A. Lane, X. Qian, S. Nie, Chem. Rev. 2015, 115, 10489.

[22] J. Dong, P. L. Carpinone, G. Pyrgiotakis, P. Demokritou, B. M. Moudgil, *KONA Powder Part. J.* **2020**, *37*, 224.

2. Comment 2: The section entitled "Biocompatibility of SERS-NPs" is incorrectly labeled. Performing cytotoxicity studies is NOT biocompatibility; this pertains to the stability of particles in a biological milieu, such as blood or serum. Please perform these studies (stability in high salt, serum pH etc....) and report the results by UV/Vis or DLS. Also, the zeta potential of the particles needs to be measured for full characterization data.

Response: Following reviewer's suggestion, we have performed stability analysis as well as zeta potential measurements under a variety of conditions including changes in salt concentrations and the presence of serum proteins. UV/Vis, DLS, and zeta potential of the particles have been added. The results are presented in **Figures S6** and **Table S1**.

Table S1. ζ potential measurements (mean \pm standard deviation, N =3).

Samples	Zeta Potential (mV)
Au NP Seed	-41 ± 2
S420 SERS-NPs	-36 ± 2
S481 SERS-NPs	-35 ± 3
PEG-S420 SERS-NPs	-22 ± 1

HA-S481 SERS-NPs	-28 ± 2
Liposome-S420 SERS-PEG	-13 ± 4
Liposome-S481 SERS-HA	-24 ± 3

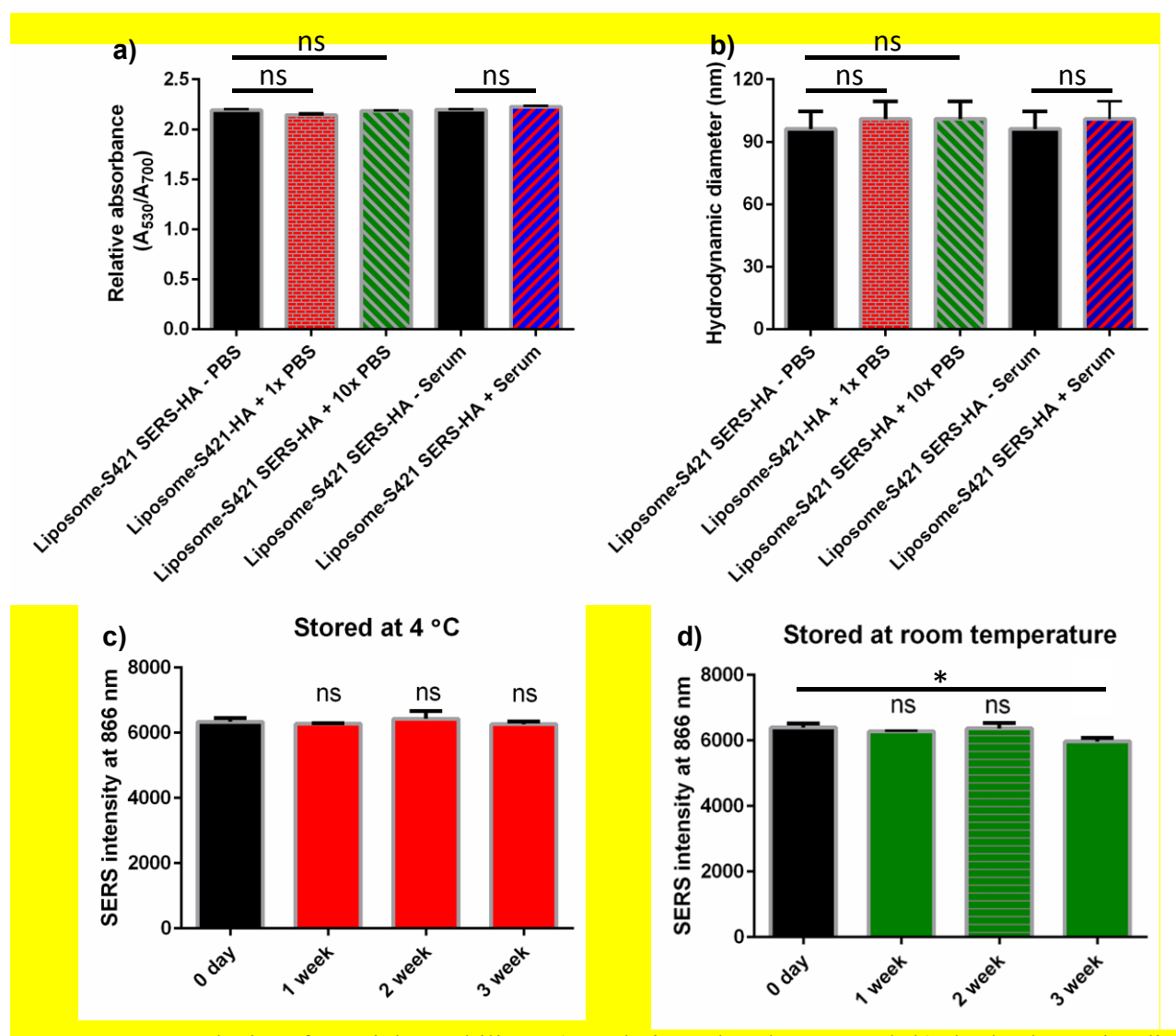


Figure S6. Analysis of particle stability. a) Relative absorbance and b) hydrodynamic diameter of the liposome-S421 SERS-HA particle in water, PBS 1x, PBS 10x, without serum (-serum), and with serum (+ serum). No statistically significant changes in the relative absorbance data or the hydrodynamic diameters suggested the stability of the NPs in PBS and serum. SERS signal intensities of liposome-S421 SERS-HA stored at c) 4 °C or d) room temperature over time. For each column, the mean value with the standard deviation was plotted. For each concentration, the values were from three samples. No statistically significant change in SERS intensity was observed for the NPs stored at 4°C up to 3 weeks. NPs stored at room temperature showed some changes in SERS intensities only at the 3-week mark. Statistical analysis was performed using a two-way ANOVA. ns: P > 0.05. *: P < 0.05.

3. Comment 3: The issues the authors had with the synthesis of some of the nanoparticles is very curious. There are a host of studies where Raman dyes were coated on AuNPs followed by coating with silica to stabilize the dyes on the metal surface. It is curious why this method did not work here since the methods here are not different from other studies??

Response: The silica coating of AnNPs was successful in our hand. However, we observed significantly reduced SERS intensities following the coating. The decrease in SERS signal intensities following silica coating has been reported by others (Refs # 9; 49) While the exact reason for the decrease is not known, it is likely due to the displacement of SERS dye from NP surface due to silica coating.

- [9] N. D. Israelsen, C. Hanson, E. Vargis, *Sci. World J.* **2015**, *2015*, 124582 and references cited therein [49] Y. Zhang, X. Li, B. Xue, X. Kong, X. Liu, L. Tu, Y. Chang, *Sci. Rep.* **2015**, *5*, 14934.
- 4. Comment 4: The authors make the point that a reason to use HA is due to the expense and stability of monoclonal antibodies. While it is true that commercially available mAb are expensive, they can also be prepared recombinantly for lower prices. In addition, their long-term stability is rather good, as many of them are, as is well known, used clinically with great success in tumor therapy. Thus, I feel this "drawback" of mAbs should be toned down slightly. I agree that using an inexpensive polysaccharide is a worthy substitute, however, CD44 is also expressed on many normal cells (including stem cells) and is important in many cell adhesion and wound healing processes. A control with binding to normal cells expressing CD44 in the process of tumor therapy would be a useful comparison.

Response: We have toned down the discussion on drawback of mAbs. The reviewer is right that CD44 is also found on normal cells. CD44 is known to exist in three forms, the low affinity form, the inflammation-induced high affinity form, and the constitutively high affinity form. In normal cells, CD44 primarily exists in the low affinity form only with weak affinities toward HA binding. In contrast, CD44 is found to be in its constitutively highly affinity form on tumor cells. This discussion has been added to the manuscript as the following.

While antibodies can bestow high specificity in target binding, they can be expensive especially for pre-clinical studies (hundreds of \$ per 100 µg) and can denature upon extended storage. Although the cost of monoclonal antibodies can be potentially managed with wide clinical adaption, as an alternative, we explored polysaccharides such as HA^[34] as the targeting ligand. HA is readily available commercially (~\$200/g), can be stored for extended periods, and is biocompatible as highlighted by its common usage in the cosmetic industry. A major receptor of HA in human bodies is the glycoprotein CD44. ^[35] On normal cells, CD44 exists primarily in the inactive low affinity form exhibiting minimal binding with HA, ^[36] which can be converted to the active high HA affinity structure in the presence of inflammatory signals. ^[37] In contrast, tumor-derived cells often express CD44 in its high-affinity state capable of constitutively binding HA, ^[38] and the high affinity CD44 is found over-expressed on the surfaces of a wide range of cancer cells. ^[39-41]

5) Comment 5: It is also curious that the HA NPs stick to the surface of the liposomes in that formulation and are so much better at binding CD44. One would think that the interaction between lipid and HA may hinder that interaction. And the fact that the thiolated HA did not result in much addition of HA to the AuNP-SERS surface is also curious, as many polysaccharides that bind to AuNP surfaces tend to stabilize these constructs by "wrapping" around the gold surface with the sugar polymer making them more biocompatible. I think more explanation about the results of the synthesis are warranted.

Response: We thank the reviewer for the question. It is interesting that the liposomal formulation of HA SERS-NP gave significantly stronger binding to CD44. HA is known to interact with phospholipid as well besides the SERS-NP. It is possible that with the liposomal formulation, more HA can be attached leading to enhanced avidity with CD44.

It is known that HA can interact with phospholipids through hydrogen bonding and hydrophobic interactions with HA distributed in punctate patterns on lipid bilayer surface. [58-59]

6) Comment 6: When the issue of the various "flavors" of resonant, and non-resonant dyes comes up, I strongly feel that the structures should be in the main text of the manuscript, not in the SI. The author needs to

see the structures that the authors are working with while reading the results section. They can, of course, remain in the SI, but they also need to be in the main text. And importantly, why did the authors use both bipyridyl and a fully deuterated analogue? Is this standard practice in SERS work? If it is, please add a sentence or two as to why these two are compared (for the uninitiated). I understand that H-D exchange can be detected by SERS, but why it is used here is unclear.

Response: We thank the reviewer for this suggestion. The structures of the dyes have been added to the main text as figure 1f.

The reason S420 and S421 (deuterium containing version of S420) are used is because they have distinctive Raman peaks (Figure 2a) helping to increase the number of dyes can be used. The following explanation has been added to the text.

Despite similarity in structures of some Raman dyes (for example S420 vs S421), these dyes have distinct fingerprint patterns in their respective Raman spectra potentially enabling multiplexing (**Figure 2a**).

7) Comment 7: There is a distinct lack of controls in the tumor work. While I understand that the authors are using the liposome-SERS-Peg particles as "non-targeting" controls, they also need to employ another tumor line which is known to not express CD44 as well as a normal line. There are other molecules that HA may bind to and this needs to be done side-by-side with tumor such as 4T1. The experimental section describing the guided imaging has no description of how in the Polyoma Middle-T antigen MMTV mice were generated: Were they purchased? Obtained as a gij? Also, that section states "A MUC1/MMTV mouse...." What is a MUC1/MMTV mouse? Are there mutant mucins involved such as MUC1? There needs to be a much more detailed description of this model and an explanation of why there is a "MUC1" in the description?

This is a nice paper, but some issues need to be resolved before publication.

Response: We thank the reviewer for the suggestions. It is true that there are other receptors such as HA receptor for endocytosis (HARE), lymphatic vessel endothelial hyaluronan receptor 1 (LYVE-1) for HA besides CD44. However, these receptors are typically not found at tumor site as HARE is mainly expressed in liver and LYVE-1 is mainly found in lymphatic vessels. For the application of HA NPs in image guided surgery, they should not post much interference.

As the NPs are targeting CD44 overexpressed on tumor cells, they are not suitable to detect CD44 negative tumor. We have added the discussion on this limitation in the main text as the following:

There are limitations to our study. While many breast cancer cells express CD44,^[39, 73] due to tumor heterogeneity, it is possible that there are cancer cells with low or no expression of CD44, which will not be detected using our approach. For more comprehensive cancer detection, biomarkers beyond CD44 can be targeted. With the potential for multiplexing, the SERS-NP strategy can be applied for simultaneous detection of multiple biomarkers in one imaging session, which is a direction we will pursue.

We have added the source and more information on the Polyoma Middle-T antigen MMTV mice. We apologize for the mentioning of MUC1, which was a mistake and has been corrected.

MMTV-PyMT transgenic mice were purchased from the Jackson Laboratory. In a span of 4 months, the female mice showed the spontaneous onset of palpable breast cancer. The mice were housed at Michigan State University's Laboratory Animal Resources Facility. All activities and protocols related to the animal study received approval from the Institutional Animal Care and Used Committee (IACUC) at Michigan State University.

Reviewer 2

1. **Comment 1**: The authors have reported a fairly novel one-pot synthesis of a stable SERS-NP that is colloidally linked to hyaluronic acid (HA) which would then specifically target CD44, a marker that is prominent in many cancers and in T-lymphocytes of inflammatory cells. If this technology is feasible and is relatively non-toxic then, the field has developed one more tool in detecting tumor and perhaps tumor margins in a surgical and post-tumor resection setting.

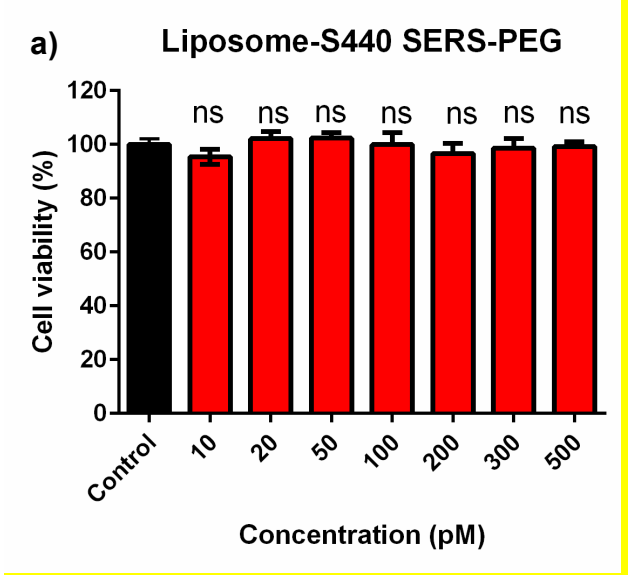
Response: We thank the reviewer for the positive feedback.

2. Comment 2: We are not in the position to rigorously review the chemical synthesis and characterization of the liposome-based HA-SERS-NP. However, it would have been nice if we had seen more stability data through DLS measurements using the Zetasizer or through examination of the stability of the Raman spectra over time or both? Do electron microscopy studies show changes in aggregations with respect to time of initial synthesis or with respect to storage temperature?

Response: We thank the reviewer for the suggestions. We have performed additional stability studies. The additional results including DLS, zeta potential and stability over time are now presented in Table S1 and Figure S6. There were not significant changes in particle sizes with respect to time or storage temperature. Please see response to reviewer 1 comment 2.

3. Comment 3: I also have some questions as to how they conducted their toxicity and preclinical safety studies. I noticed that the MTS assay for in vitro cellular viability when challenged with the SERS-NP was on Raw 264.7 cells (Figure S4) (a macrophage cell line?). No toxicity was reported up to 100 pM. It would have been nice to see a fuller toxicity/dose response study where an actual LD50 number was obtained. Also aside from the MTS study, we do not see the Raw 264.7 cells again in the report. The authors focus primarily on 4T1 cells to study NP specificity (Figure 4) and I think they use the MUC1/MMTV mouse models to examine in vivo/preclinical uptake of surgical-guided SERS-NP-HA onto spontaneous tumors (Figure 5). Thus it is unclear, how generalizable across different cancer cell lines are the safety and specificity data they present on their SERS-NP. Indeed, it is not clear in their studies how specific are their NPs are to cancer cells as opposed to inflammatory cells. This will become important even in their limited application of a post-resection setting as the tumor microenvironment often is populated with inflammatory immune cells.

Response: We thank the reviewer for the questions. To be consistent, we have performed additional cell viability studies with 4T1 breast cancer cells (**Figure S4**). The particles did not significantly affect the cell viability up to 500 pM. Typical concentrations of the NP used for *in vitro* and *in vivo* experiments were below 250 pM. For the MTS viability assay, we were not able to get to higher NP concentrations as the NP is also colored and would interfere with the optical absorbance reading in MTS assay at higher NP concentrations.



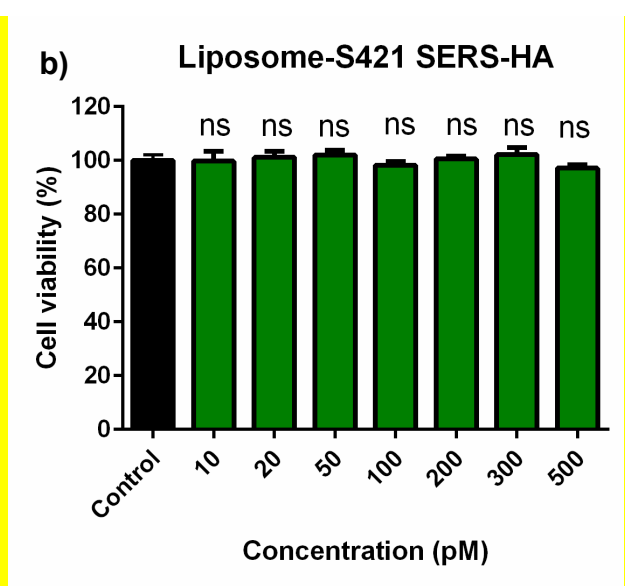


Figure S4. MTS assays with 4T1 breast cancer cells indicated the NPs did not affect the cell viabilities under the experimental condition. 4T1 cells were incubated with a) liposome-S440 SERS-PEG or b) Liposome-S421 SERS-HA for 4 h under various NP concentrations: 0 pM, 10 pM, 20 pM, 50 pM, 100 pM, 200 pM, 300 pM, and 500 pM. No significant changes in cell viability were observed suggesting the NPs were not toxic to cells up to at least 500 pM. For each column, the mean value with the standard deviation was plotted. For each concentration, the values were from three samples. Statistical analysis was performed using a two-way ANOVA. ns: P > 0.05.

As discussed in responses to Reviewer 1's comment 7, CD44 on normal cells are typically in a low affinity state, with little binding to HA. Thus, the SERS-NP-HA can readily differentiate normal cells vs CD44 expressing tumor cells. Our NP probes selectively target CD44, which will not bind with CD44 negative tumor cells. This is a limitation of the current study, which has been discussed in the text as the following:

There are limitations to our study. While many breast cancer cells express CD44,^[39, 73] due to tumor heterogeneity, it is possible that there are cancer cells with low or no expression of CD44, which will not be detected using our approach. For more comprehensive cancer detection, biomarkers beyond CD44 can be targeted. With the potential for multiplexing, the SERS-NP strategy can be applied for simultaneous detection of multiple biomarkers in one imaging session, which is a direction we will pursue.

The reviewer is right that some inflammatory cells can bind with CD44. In the tumor microenvironment, immune cells can infiltrate into tumor tissues and be mixed with cancer cells. Therefore, for complete elimination of tumor at the tumor site, it is common to surgically remove the infiltrated immune cells together with tumor. As the NPs are applied only locally to the tumor site in our application, only cells in the tumor site will be removed. Thus, the imperfect selectivity of tumor vs immune cells is not a significant drawback.

In summary, we are very grateful for reviewers' comments, which help us develop a stronger manuscript. With the revisions made, I hope the paper can now be accepted. If you would require any further information, please do not hesitate to contact us.

Sincerely,

Xuefei Huang, Ph. D. Department of Chemistry Michigan State University East Lansing, MI 48824-1322

1						
2						
1 2 3 4 5	1	Robust Synthesis of Targeting Glyco-nanoparticles for Surface Enhanced Resonance Raman				
6	6 2 Based Image-Guided Tumor Surgery					
7 8 9	Kunli Liu, a,b,# A. K. M. Atique Ullah, a,b,# Aniwat Juhong, b,c Chia-Wei Yang, a,b Cheng-Yo					
10 11	4	Yao, b,c Xiaoyan Li,d Harvey L. Bumpers, Zhen Qiu,b,c,f* Xuefei Huanga,b,f*				
12 13	5	^a Department of Chemistry, Michigan State University, East Lansing, MI, 48824 USA				
14	6		ealth Science and Engineering, Michigan State University, East			
15 16	7	Lansing, MI, 48824 USA				
17	8	-	d Computer Engineering, Michigan State University, East Lansing,			
18 19	9 10	MI, 48824 USA	vironmental Engineering, Michigan State University, East Lansing,			
20	11	MI, 48824 USA	whomhental Engineering, whemgan State Oniversity, East Lansing,			
21	12		chigan State University, East Lansing, MI, 48824 USA			
22 23	13		Engineering, Michigan State University, East Lansing, MI, 48824			
24	14	USA				
25 26	15	#Equal contribution	20			
27	16	Email: <u>qiuzhen@msu.edu</u> ; <u>h</u>	uangxu2@msu.edu			
28 29	17	ORCID:				
29 30	1 /	okeib.				
31	18	Kunli Liu	0000-0003-1954-9776			
32 33						
34	19	A. K. M. Atique Ullah	0000-0002-4545-2663			
35	20	August Teller	0000 0002 0115 0767			
36 37	20	Aniwat Juhong	0000-0002-9115-9767			
38	21	Chia-wei Yang	0000-0002-0950-5510			
39 40		cina wor rung	0000 0002 0200 2210			
41	22	Cheng-you Yao	0000-0002-6045-8676			
42						
43 44	23	Xiaoyan Li	0000-0002-2649-7575			
45	24	Howard Dames	0000-0001-6165-9261			
46 47	24	Harvey L. Bumpers	0000-0001-0103-9201			
48	25	Zhen Qiu	0000-0001-8790-8481			
49						
50 51	26	Xuefei Huang	0000-0002-6468-5526			
52						
53 54	27					
55	28					
56						
57 58						
59						
60						
61 62						
63						
64 65						
00						

Keywords: glyco-nanoparticles, imaging guided surgery, surface enhanced Raman spectroscopy, synthesis

Abstract

Surface Enhanced Resonance Raman (SERS) is a powerful optical technique, which can help enhance the sensitivity of Raman spectroscopy aided by noble metal nanoparticles (NPs). However, current SERS-NPs are often suboptimal, which can aggregate under physiological conditions with much reduced SERS enhancement. Herein, a robust one-pot method has been developed to synthesize SERS-NPs with more uniform core diameters of 50 nm, which is applicable to both non-resonant and resonant Raman dyes. The resulting SERS-NPs are colloidally stable and bright, enabling NP detection with low-femtomolar sensitivity. An algorithm has been established, which can accurately unmix multiple types of SERS-NPs enabling potential multiplex detection. Furthermore, a new liposome-based approach has been developed to install a targeting carbohydrate ligand, i.e., hyaluronan, onto the SERS-NPs bestowing significantly enhanced binding affinity to its biological receptor CD44 overexpressed on tumor cell surface. The liposomal HA-SERS-NPs enabled visualization of spontaneously developed breast cancer in mice in real time guiding complete surgical removal of the tumor, highlighting the translational potential of these new glyco-SERS-NPs.

Introduction

Raman spectroscopy is an attractive optical technique to simultaneously detect multiple targets of interest. However, the low inherent sensitivity of Raman hinders its wide application. To overcome this drawback, Raman active dyes can be deposited onto noble metal surface. An up to 10 orders of magnitude enhancement of Raman signals can be potentially observed, which is referred to as Surface Enhanced Resonance Raman (SERS). Au-nanoparticles (Au-NPs) coated with Raman dyes have been one of the most popular types of SERS-NPs investigated, which have been applied in many areas, including chemical analysis, environmental monitoring, and medical diagnostics.

To prepare Au based SERS-NPs, the Au-NP cores have been most commonly synthesized *via* the sodium citrate reduction method,^[6] which was followed by the absorption of Raman active probes onto the NP surface.^[4, 7-8] As the core sizes of Au-NPs are known to significantly impact Raman signal enhancement,^[9-10] it would be ideal that the SERS-NPs synthesized have narrow size distributions. Furthermore, the NPs should be stable in biological media, which tend to foul the surface of the particles resulting in NP aggregation and significantly reduced SERS properties. Methods that can generate bright and colloidally stable SERS-NPs with uniform size and shape distribution are important.^[1-2, 4, 11-12]

For biological detections aided by SERS-NPs, another important parameter is the selective binding of NPs to the target of interests.^[13] In order to accomplish this, ligands such as monoclonal antibodies can be conjugated to NP surface to aid in targeting.^[14-15] Several strategies have been developed to install targeting ligands including through the high affinity interactions of gold and sulfhydryl group^[16] or coating of the NP with a layer of silica to introduce reactive functional groups onto the NP surface.^[17] For example, recently, the impressive synthesis of a library of 26 gold-based SERS-NPs has been reported, which aided in the detection of multiple types of tumor cells.^[17] On the other hand, with the high cost and the relative ease of denaturing of monoclonal antibodies, other types of targeting ligands can be explored.

Herein, we report a synthetic strategy to prepare bright and colloidally stable SERS-NPs, which is applicable to a wide range of Raman dyes (flavors). An algorithm has been adapted to decode the resulting library of SERS-NPs with multiple flavors through their respective characteristic Raman fingerprints. Furthermore, as an alternative to monoclonal antibodies, a readily available carbohydrate, i.e., hyaluronan (HA) has been investigated as the targeting ligand

on SERS-NPs. However, the direct attachment of HA onto SERS-NPs failed to produce significant targeting of the biological receptor, CD44 protein, overexpressed on tumor cells. To overcome this obstacle, a new liposomal based synthesis approach has been established that led to a new type of HA-SERS-NP with significantly enhanced CD44 binding. The liposomal HA-SERS-NP can effectively guide the complete surgical removal of breast cancer spontaneously developed in mice in real time through Raman imaging, highlighting its translational potential.

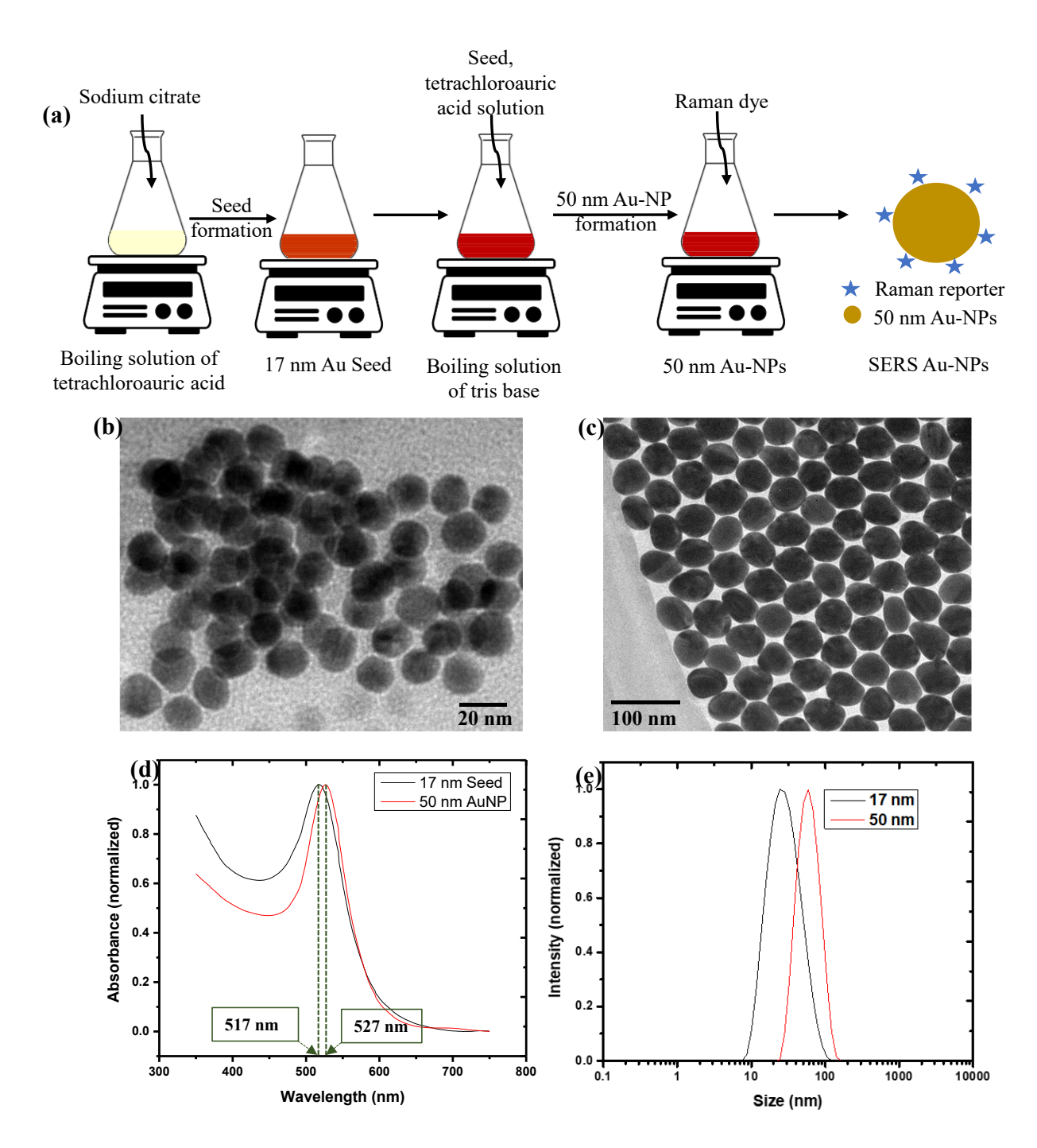
Results and discussion

Development of a robust synthesis protocol for SERS-NPs

Our synthesis of SERS-NPs started from the formation of Au-NP cores followed by coating with a Raman active dye. The first synthetic approach we tested utilized the common method of sodium citrate reduction of tetrachloroauric(III) acid to prepare NPs with an average of 50 nm diameter.[18-19] The Au-NPs formed were then incubated with a non-resonant Raman dye such as S420.^[18] However, these NPs gave little SERS signals at pM NP concentration, which was presumably because of the low amounts of dye attached to the Au-NPs with this synthetic procedure in our hands. To improve the SERS intensities, a variety of synthetic conditions was examined, [20] which included varying the timing of dye addition vs the formation of Au-NPs, and the addition of additives such as ammonia hydroxide to stabilize Au-NPs formed before the installation of the Raman dye. However, none of these efforts yielded stable NPs with strong SERS signals.

Another complication observed in the synthesis was the inhomogeneity of the NP core formed. It is known that the optimal core diameters of the Au-NPs around 50 nm are ideal for maximum SERS enhancement.^[10] When Au-NPs synthesized were larger than 30 nm through the sodium citrate reduction method, significant heterogeneities in shape and size of Au-NPs were observed (Figure S2), which were consistent with literature reports.^[21-22]

The aforementioned difficulties encountered in SERS-NP synthesis prompted us to examine alternative procedures. While there are many methods for the preparation of Au-NPs, [21, ^{23-30]} only a few of them have been applied to the formation of SERS-NPs with strong SERS signals applicable to multiple Raman dyes. After exploring various synthesis strategies, the seed mediated growth method with tris base^[31] (**Figure 1**) turned out to be the best in our hands.



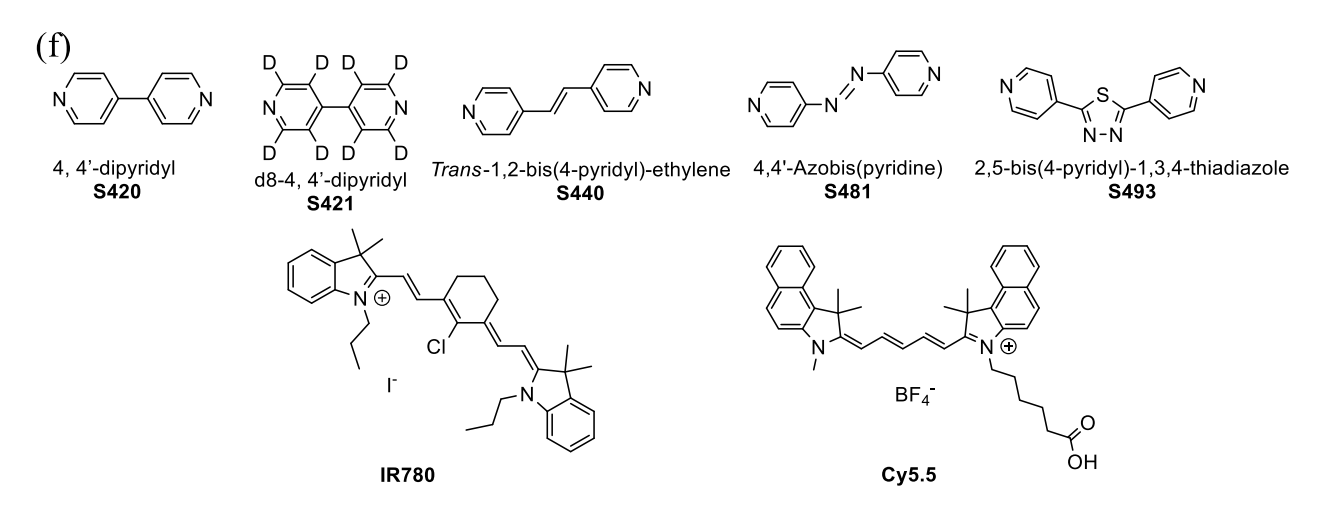


Figure 1. Synthesis and characterizations of SERS-NPs. (a) Schematic illustration of the tris base assisted synthesis of SERS-NPs. Au-NP seeds were first produced via the sodium citrate reduction method, which was followed by seed mediated growth via tris base leading to 50 nm Au-NPs at 100 °C. The Raman dye was added right after the formation of 50 nm Au-NPs and stirred for 1 minute, followed by immediate cooling down in an ice bath. This method was applicable for both non-resonant and resonant dyes yielding bright SERS signals with the concentrations of dyes needed differing significantly between non-resonant dyes (10 µM) and resonant dyes (50 nM). TEM images of (b) Au-NP seeds and (c) SERS-NPs. (d) UV-vis spectra and (e) hydrodynamic diameters of Au-NP seeds and SERS-NPs in MilliO water at room temperature. f) Structures of non-resonant dyes (S420, S421, S440, S481, and S493) and resonant dyes (IR780, and Cy5.5) examined for SERS-NP formation.

For the seed mediated growth strategy, Au-NP seeds with average diameters of 17 nm were synthesized first with sodium citrate as the reducing agent. The Au-NP seeds were then mixed with a solution of tris base heated at 100 °C followed by the addition of tetrachloroauric acid, which triggered NP growth to form 50 nm Au-NPs by tuning the number of seeds vs the amount of tetrachloroauric acid added. To install the Raman dye, we discovered that upon formation of the 50 nm Au-NPs, a dye such as S420 (10 µM) should be immediately added to the NP solution at 100 °C. The resulting SERS-NPs were stable in solution and gave bright Raman signals. The schematic illustration of the synthesis of SERS-NPs was shown in Figure 1a. Addition of the dye after the Au-NP solution had cooled down, before or during seeded growth of the NPs, failed to produce SERS-NPs with strong Raman signals. Thus, the small-time window for Raman dye

installation right after the formation of Au-NPs is critical, presumably because the nascent Au-NP surface has a significant number of vacant sites for the Raman dye to bind. Au-NP seeds and SERS-NPs were characterized by UV-vis spectroscopy, transmission electron microscopy (TEM), dynamic light scattering (DLS), and ζ potential analyses (Figures 1b-1e and Table S1). These SERS-NPs were more homogeneous in size distribution with average diameters of 50 nm compared to those prepared directly via the citrate reduction method (Figure 1c and Figure S2). The surface plasmon resonance (SPR) bands observed at 517 nm and 527 nm were also an indication of the formation of 17 nm Au-NP seeds and 50 nm SERS-NPs respectively (Figure 1d). [32] The size distribution of the 50 nm SERS-NPs prepared *via* the seed mediated synthesis was further validated from their hydrodynamic size measured by dynamic light scattering analysis (Figure 1e). The ζ potentials of the SERS-NPs were around -35 mV, which was more positive than that of the NP seed (- 41 mV) presumably due to the displacement of negatively charged sodium citrate from NP surface by tris base (Table S1).[31]

The generality of our synthesis procedure for both non-resonant and resonant Raman dyes was investigated. SERS-NPs bearing non-resonant Raman dyes^[33] S420, S421, S440, S481, and S493 (Figures 1f and S1) respectively showed strong SERS Raman signals. Despite similarity in structures of some Raman dyes (for example S420 vs S421), these dyes have distinct fingerprint patterns in their respective Raman spectra potentially enabling multiplexing (Figure 2a). For resonant Raman dyes (dyes with absorbance overlapping with the wavelength of the incident light) such as IR780, interestingly, when 10 µM of the IR780 dye was used as for the non-resonant dye, it led to instantaneous aggregation of Au-NPs. Upon careful optimization, it was discovered that 50 nM of IR780 was sufficient to produce bright NPs. This supported the idea that with the extended conjugated structure, a resonant Raman dye can have a higher affinity to Au-NPs as compared to a non-resonant Raman dye. Besides IR780, resonant Raman dyes IR792 and Cy5.5 also produced NPs with strong signals with IR792 giving similar SERS spectrum as that of IR780.

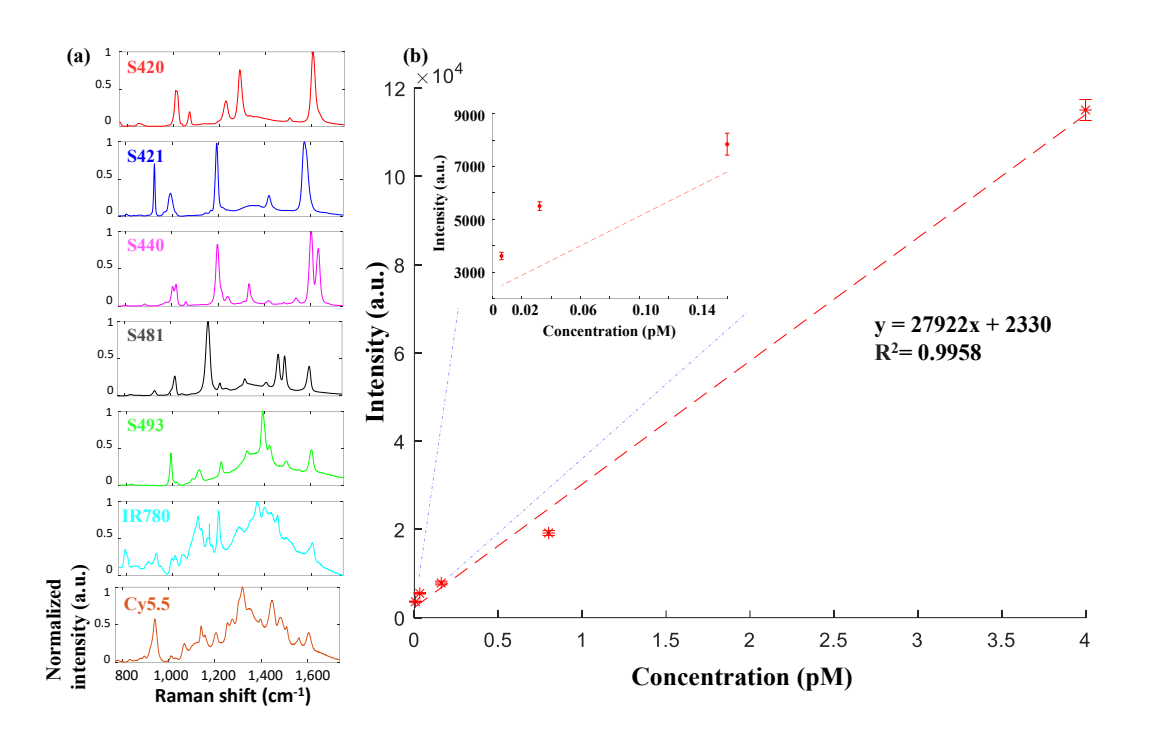


Figure 2. (a) Raman spectra of SERS-NPs (S420, S421, S440, S481, S493, IR780, and Cy5.5). (b) The intensities of the highest peaks of Raman spectra of SERS (S440)-NP correlated linearly with NP concentrations. The insert in the figure shows that SERS (S440)-NP can be sensitively detected at low fM concentrations.

Detection limit analysis and ratiometric quantification of mixtures of various flavors of **SERS-NPs**

Detection limits of the SERS-NPs synthesized were evaluated. The intensities of Raman signals from solutions (200 pM, 100 pM, 20 pM, 4 pM, 800 fM, 160 fM, 32 fM, and 6 fM) containing various flavors of SERS-NPs (S420, S421, S440, S481, S493, IR780, and Cy5.5 (Figure 1f)) were measured. These Raman dyes were selected due to their distinct Raman signals and commercial availabilities. As shown in Figure 2b, even at 6 fM concentration, NP such as S440 SERS-NP could still be detected.

An important application of the SERS-NPs is to use a library of SERS-NPs to detect multiple targets simultaneously. In order to accomplish this, an unmixing algorithm needs to be established. Phantoms with mixtures of three flavors of SERS-NP at seven different ratios of the SERS-NPs were prepared (Figure S3a). Three sets of spectra were acquired: 1) spectra of the solutions of various mixed NPs; 2) the reference spectrum for each flavor; and 3) background

spectra, i.e., the spectra of the plastic tube container filled with water. Codes were prepared and applied to demultiplex the components, which accurately determined the ratios of the various flavors of the particles in the mixture (Figure S3b).

Ligand attachment to SERS-NPs

For biological detection, it is desirable that targeting ligands can be attached to the SERS-NPs. The most common ligand type investigated for SERS-NPs to date is monoclonal antibodies.[17] While antibodies can bestow high specificity in target binding, they can be expensive especially for pre-clinical studies (hundreds of \$ per 100 µg) and can denature upon extended storage. Although the cost of monoclonal antibodies can be potentially managed with wide clinical adaption, as an alternative, we explored polysaccharides such as HA^[34] as the targeting ligand. HA is readily available commercially (~\$200/g), can be stored for extended periods, and is biocompatible as highlighted by its common usage in the cosmetic industry. A major receptor of HA in human bodies is the glycoprotein CD44. [35] On normal cells, CD44 exists primarily in the inactive low affinity form exhibiting minimal binding with HA, [36] which can be converted to the active high HA affinity structure in the presence of inflammatory signals.^[37] In contrast, tumor-derived cells often express CD44 in its high-affinity state capable of constitutively binding HA, [38] and the high affinity CD44 is found over-expressed on the surfaces of a wide range of cancer cells.^[39-42] HA has been conjugated to a variety of NPs for imaging applications such as magnetic resonance imaging and fluorescence^[43-46] or in vitro enzyme detection.^[47] However, to the best of our knowledge, it has not been utilized for in vivo SERS-NP based detection.

To attach HA on SERS-NPs, the first approach attempted was to coat SERS-NPs with a layer of silica to introduce functional groups such as amine onto NPs.^[18] The Stöber method is one of the most common approaches for silica coating on NPs through the hydrolysis of tetraethoxysilane (TEOS) with ammonia hydroxide as the base. [48] However, in our synthesis, the addition of ammonia hydroxide to promote the silica formation on NPs significantly reduced SERS signals of the resulting NPs presumably due to desorption of Raman dye from NPs in the process. Increasing the concentration of the Raman dye to 1 mM during TEOS coating of SERS-NPs did not improve the Raman signals. While silica coated SERS-NPs have been reported, [17, 49] our results are consistent with the findings that silica coating can significantly reduce SERS intensities.[9, 50]

⁴ 209

8 211

10 212

16 17 216

217

223

224

228

58 239 59 239

21 218 22 210

235

As an alternative to silica coating to attach biomolecules to Au-NP surface, ligands can be functionalized with sulfhydryl groups by taking advantage of the strong gold-thiol interactions.^[51-55] HA (average MW: 10 kDa) was thiolated and incubated with the SERS-NPs overnight followed by repeated centrifugation to remove unbounded HA.

Colloidal stability of NPs is important for biological applications. While the uncoated SERS-NPs were readily dispersed in water, these particles aggregated in PBS buffer as evident from the precipitation observed and the loss of color in the supernatant (Figures S4ai vs S4aii). HA coating of SERS-NPs significantly improved the colloidal stability of the particles with HA-SERS-NPs stable in PBS buffer with no precipitation for more than six months (Figure S4aiii). Consistent with HA installation, there was an increase in the hydrodynamic diameter and change in the ζ potential of the HA-SERS-NPs as compared to the uncoated SERS-NPs (Figure S4b and Table S1). To confirm that HA immobilized retained their biological binding, a competitive enzyme linked immune-sorbent assay (ELISA) was set up, [56-57] where the HA-SERS-NPs were used to compete against native HA polysaccharide for binding with immobilized CD44 in ELISA wells (Figures S4c and S4d). As SERS-NPs are often applied at relatively low concentrations (pM), the HA-SERS-NPs formed with this direct coating method were assayed up to 250 pM concentrations. However, these HA-SERS-NPs showed relatively weak affinities for CD44 as evident from the significant (~50%) CD44 binding remaining even with 250 pM of SERS-NPs (Figure S4d). To test the possibility that Raman dye installed on the SERS-NPs interfered with HA binding, thiolated HA was also incubated with Au-NPs without Raman dye. The resulting NPs did not have stronger binding with CD44 in the competitive ELISA assay either (Figure S4e). The usage of higher molecular weight HA (MW: 250 kDa and 1,500 kDa) for NP coating did not lead to improvement in binding (Figure S4e). The weak avidity of such HA-NPs with CD44 was presumably due to the insufficient amounts of HA immobilized on NP surface.

We explored various methods to enhance the affinity of SERS-HA-NPs with CD44. We envision that stronger binding may be achieved with higher loading of HA on the NPs. To accomplish this, we explored liposomal formulation^[58] of SERS-NPs, which have not been investigated before. The thin-film hydration method was applied first using a solution of SERS-NPs to hydrate the lipid film. However, extensive NP aggregation was observed during the hydration process, as indicated by the color change to black. To overcome this, SERS-NPs were incubated with thiolated HA (HS-HA) first, which were then used to hydrate the lipid film (**Figure**

 3a). No significant absorbance change or aggregation (via UV-vis absorption and hydrodynamic diameter) was observed for liposome-SERS-HA after 24 h of incubation (Figure S5) in PBS and serum. Thus, the resulting liposome-SERS-HA were colloidally stable in PBS buffer and serum. As a control, thiolated polyethylene glycol (PEG-SH, MW 5 kDa) was immobilized onto SERS-NPs following the same liposomal formulation strategy as liposome-SERS-HA (Figure 3a). The TEM images of the SERS-NPs before and after the liposomal complex formation showed that SERS-NPs were bound on the surface of liposome (Figures 3b-e). The formation of liposomal complexes was evidenced from the increase of the hydrodynamic diameter (Figure 3f) and change in ζ potential (**Table S1**). Interestingly, this new liposome-SERS-HA exhibited strong CD44 binding in the competitive ELISA assay with the avidity of CD44 significantly improved compared to the HA-SERS-NPs formed without liposome formulation as 15 pM of liposome-SERS-HA almost completely inhibited HA binding with CD44 with a dose dependent response (Figures 3g and 3h vs Figure S4d). HA thiolation was important as liposome-SERS-NPs obtained with the non-thiolated HA did not compete against HA for CD44 binding (Figure 3g). It is known that HA can interact with phospholipids through hydrogen bonding and hydrophobic interactions with HA distributed in punctate patterns on lipid bilayer surface. [59-60] The sulfhydryl groups in thiolated HA may cluster HA around SERS-NPs on the liposomes enhancing the avidity with CD44. Under the same experimental conditions, liposome-SERS-PEG exhibited no competition against HA in the competitive ELISA assay either, highlighting the important role of HA for SERS-HA binding with CD44 (Figure 3h).

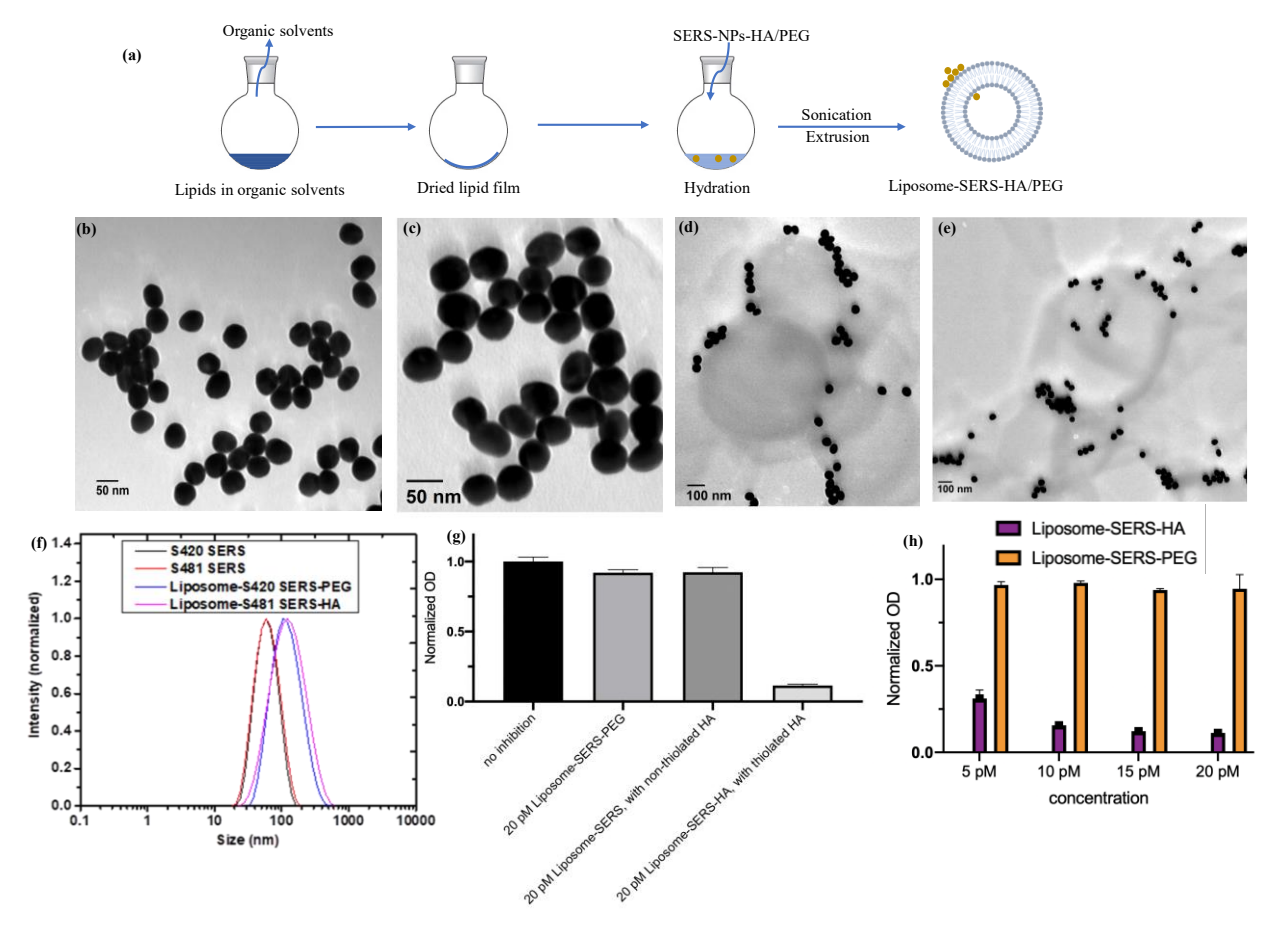


Figure 3. Synthesis and characterizations of liposome-SERS-HA and liposome-SERS-PEG. (a) Schematic illustration of the synthesis of liposome-SERS-HA/PEG. TEM images of (b) S420 SERS-NP, (c) S481 SERS-NP, (d) liposome-S420 SERS-PEG, and (e) liposome-S481 SERS-HA. SERS-HA/PEG NPs were anchored on the surface of the liposome. (f) DLS data of SERS-NPs and liposome-SERS-HA/PEG. The increased size is an indication of liposome anchoring. (g) Competitive ELISA showed that HA attachment was successful only with thiolated HA. Strong competition was observed at 20 pM liposome-SERS-HA. (h) Liposome-SERS-HA could compete against HA for CD44 binding in a dose dependent manner from 5 pM to 20 pM, while the corresponding liposome-SERS-PEG showed no effects at the equivalent concentrations. The error bars represent the standard deviations from three experiments.

The amount of HA on the liposome-SERS-HA was quantified. Comparison of the CD44 binding by liposome-SERS-HA vs HA polymer showed that 20 pM of liposome-SERS-HA contained an equivalent of 2.2 µM HA, which corresponded to 18% w/w. In parallel, the amount

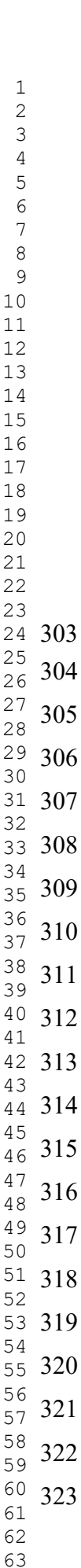
of HA attached to HA-SERS-NPs was quantified by the carbazole assay following acid cleavage of HA from the NPs, [61] which gave the average HA loading of 5%. Higher loading percentage of HA determined from the competitive ELISA assay may be due to the enhanced multi-valency effect after HA attachment to the SERS-NPs, which may be through thiol-gold interaction^[51] and HA binding to liposome. [62]

Stability and biocompatibility of SERS-NPs in biological milieu

For biological applications, it is important that the NPs are stable and biocompatible in biological milieu. *In vitro* cytotoxicity assay was performed to evaluate the toxicity of SERS-NPs in 4T1 cells. The MTS cell viability assay showed that SERS-NPs were not toxic up to the highest concentration tested (500 pM) (Figure S6). In addition, the colloidal stabilities of the SERS-NPs were examined under various conditions. As shown in Figure S5, UV-vis spectroscopy and DLS measurements of HA-SERS-NP showed little changes in nanoparticle sizes under high salt (10 x PBS) and 50% serum incubation suggesting the high stability of the particles. There were no significant changes in SERS intensities either when stored at 4°C over 3 weeks (Figure S5c).

Targeted SERS imaging of breast cancer cells

The in vitro SERS imaging of breast cancer cells was carried out using liposome-SERS-HA with liposome-SERS-PEG as the control. Breast cancer cell 4T1 was explored as the target cell, which expresses a high level of CD44 on the surface. [63-64] 4T1 cells were incubated with solutions of liposome-SERS-PEG and liposome-SERS-HA respectively under the same experimental conditions. The cells were then rinsed with the buffer to remove the unbound particles, and Raman signals were recorded. Cells incubated with liposome-S440 SERS-PEG did not show any significant Raman signals (Figures 4a-c) indicating little non-specific binding of liposome-SERS-PEG with the cells. In contrast, strong Raman signals were obtained from the cells incubated with the liposome-S421 SERS-HA (Figures 4d-f) demonstrating the binding of liposome-SERS-HA to the breast cancer cells. Similarly, other flavors of SERS-NP could also be used for the HA dependent detection of 4T1 cells demonstrating the generality (Figures S7,8).



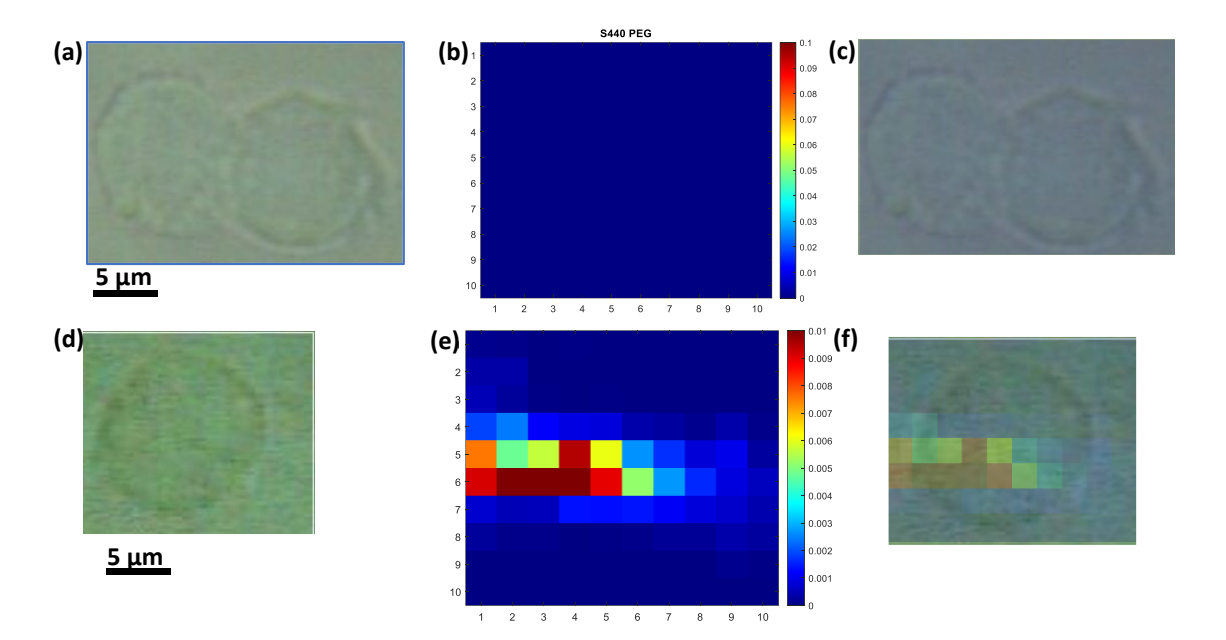


Figure 4. Images of 4T1 cells incubated with liposome-S440 SERS-PEG (panels a-c, control without targeting) and liposome-S421 SERS-HA (panels d-f. HA is used for targeting CD44 protein overexpressed in 4T1 cells) upon removal of unbound particles. (a) Bright-field microscopy image of 4T1 cells, (b) S440 SERS image of 4T1 cells, (c) overlay of a and b images. (d) Bright-field microscopy image of 4T1 cells, (e) S421 SERS image of 4T1 cells, (f) overlay of d and e images. The spectra were recorded using 50X objective lens with 10 X 10 number of pixels, 5 frames accumulation, 2 μm step size, and 1 s exposure time. Colorimetric weight factors in panel b indicated that there were no SERS signals obtained demonstrating no non-specific binding of liposome-S440 SERS-PEG by the cells was detected. In contrast, the significant signals from panel e suggest the significant binding of liposome-S421 SERS-HA with 4T1 cells.

Liposome-SERS-HA enabled successful image-guided surgery of breast cancer spontaneously developed in mice

Breast cancer is the leading cause of cancer and the second most frequent cause of death in female cancer patients. Breast conserving surgery (BCS), also referred to as lumpectomy, is the most widely used surgical procedure and standard of care for a majority of breast cancer. [65] BCS aims to completely remove the tumor while preserving surrounding healthy breast tissue. However, cancer often grows in an irregular shape, and there may be microscopic components extending from the main tumor, rendering it challenging to ensure complete tumor resection. Breast surgical oncologists typically rely on palpation and experience during surgery to determine the tumor

343 41 344

52 350

59 354

margin. Intraoperative frozen section assessment can be performed, [66] but it can significantly increase the total time needed for the operation as it is time consuming for the pathologist to evaluate the ill-defined cancer. Furthermore, some cancers are so small or nonpalpable that frozen section is not performed for fear of losing tumor specimen. After surgery, the tissues removed are commonly subject to histological analysis. If tumor is observed at the margin (termed "positive margin"), it would indicate that there is residue tumor left at the surgical sites and there are increased risks of in-breast tumor recurrence, thus necessitating additional surgery. [67] Re-excision requires a second surgical trip, additional stress to the patient, and sometime weeks before the patient can be determined to have had a cancer-free resection. The re-excision lumpectomy rate (RELR) for some individual surgeons within the United States can be as high as 70%. [68] Thus, a method that can image tumor intraoperatively and aid the surgeon to completely remove tumor without significantly increasing in-surgery time will be tremendously beneficial.

SERS-NPs have been investigated to image freshly excised mouse breast cancer tissues ex vivo to provide feedback for tumor removal. [69-70] It would be more desirable that the surgical sites can be directly imaged during surgery in real time. In addition, current studies on SERS-NPs guided surgery have only utilized xenografted mouse breast cancer model rather than the spontaneous breast cancer.[69-70]

For our study, to more closely mimic human breast cancer clinical conditions, we obtained the mouse mammary tumor virus promoter (MMTV)-polyoma virus middle T (PyMT) mice. These mice express the PyMT antigen with the MMTV promoter/enhancer. [71-72] As a result, all female PyMT/MMTV mice spontaneously develop multiple palpable mammary tumors within 4— 6 months with a more native breast cancer microenvironment and tumor morphology as compared to xenografted breast cancer.

With the tumor bearing mice, breast conserving surgery was performed by first removing the tumor surgically guided by palpating the tumor tissue area. A solution of liposome-S421 SERS-HA was then sprayed on the tumor site of resection to detect residual tumor. After 3 minutes, the surgical site was rinsed with buffer to remove unbound particles. Raman signals were observed in the tumor site. However, it was unclear to what extent the non-specific binding of NPs by the tissues played in the retention of the NPs in the surgical site.

To reduce the influence of non-specific binding and more accurately depict tumor in mice, we mixed the liposome-S440 SERS-PEG with liposome-S421 SERS-HA at 1:1 ratio. Tumor

bearing MMTV-PyMT mice were subjected to tumor removing surgery, which was followed by spraying of the mixed NP solution and removal of unbound particles through washing. After the first surgical removal of the tumor, particle spraying and washing off unbound particles, S440 signals were observed not only in part of the tumor site but also in some of the surrounding normal tissues presumably reflecting the non-specific retention of the NPs by tissues. To more precisely define the tumor location, the Raman signals from the surgical site were unmixed to calculate the ratio of the signal intensities from S421 over S440. Hotspots with significantly higher S421 signals over those of S440 in ratiometric images of the tumor would be indicative of tumor presence attributed to HA binding with CD44 expressed in tumor. After surgical removal of tumors three times, the surgical site was free of tumor signals (**Figure 5**). The tumor removed and corresponding IHC and H&E images of resected tumor were shown in **Figure 5**.

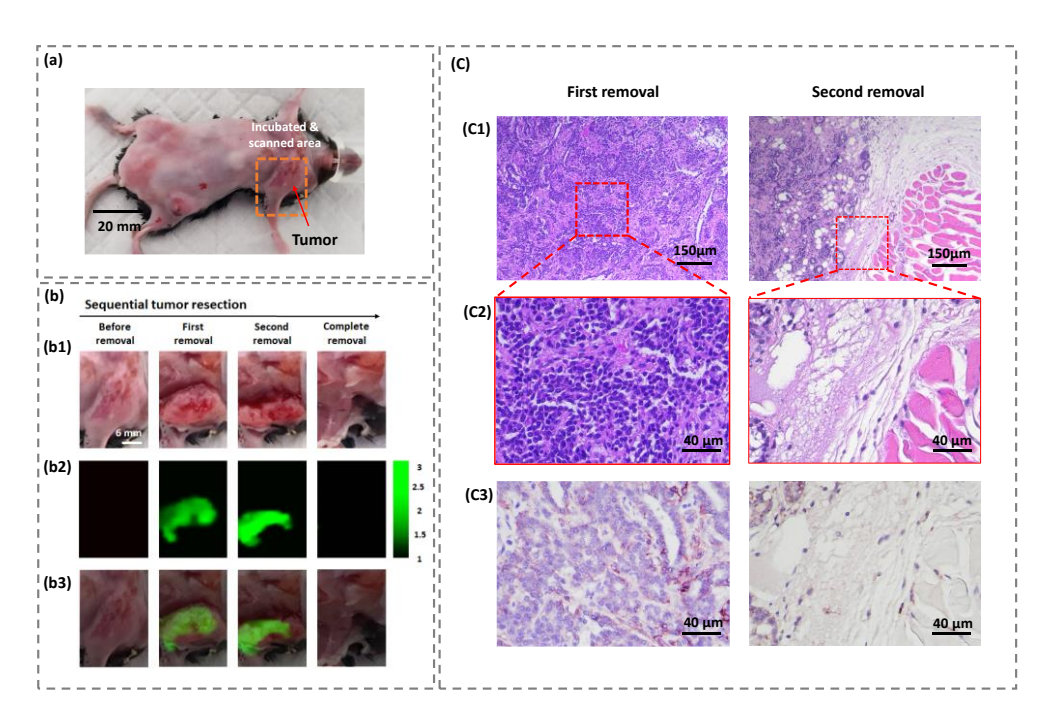


Figure 5. Raman image-guided surgery using the mixture solution of liposome-S421 SERS-HA and liposome-S440 SERS-PEG. (a) Photograph of the tumor bearing mouse before surgery; (b) Sequential tumor resection, (b1) photographs of the tumor area, (b2) the ratiometric Raman (S421/S440) images, (b3) overlaid ratiometric images with photographs the tumor areas before surgery and after each of the three surgical removal of the tumor; The scale bar is for S421/S440 weight ratio. (c) H&E and IHC images of resected tumors from (b), (c1-c2) H&E images of the

 393

 tumor acquired by 10X and 40X magnification, respectively, and (c3) the corresponding IHC images of the tumor acquired by 40X magnification.

To confirm the in vivo imaging results in mice, ex vivo staining was carried out with the surgically removed tumor, and other tissues including liver, heart, and kidney. Resected tissues were stained with a mixture of liposome-S421 SERS-HA and liposome-S440 SERS-PEG followed by repeated washing with PBS buffer to remove unbound particles. Raman imaging was performed and the ratiometric images were generated (Figure 6). Preferential accumulation of liposome-SERS-HA over liposome-SERS-PEG was observed on tumor tissue, but not in liver, kidney or heart tissue. The results from ex vivo staining corroborated with the in vivo images and the targeting ability of liposome-SERS-HA particles.

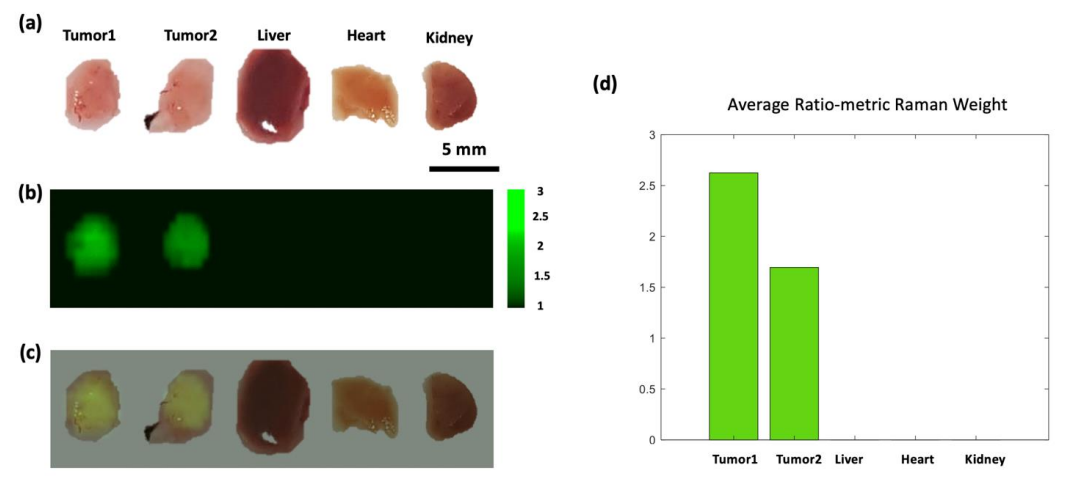


Figure 6. Ratiometric images of the mixture solution of liposome-S421 SERS-HA and liposome-S440 SERS-PEG applied on the tumor and control tissues. (a) Photograph of the tissues; (b) Ratiometric Raman images of signal intensities of S421 over those of S440; The scale bar is for S421/S440 weight ratio. (c) Overlaid images of the photograph and the ratiometric Raman images; (d) The average values of ratiometric Raman weight from various tissues. The much higher intensities from the tumor sites confirm the abilities of the liposome-S421 SERS-HA to target tumor.

There are limitations to our study. While many breast cancer cells express CD44, [39, 73] due to tumor heterogeneity, it is possible that there are cancer cells with low or no expression of CD44, which will not be detected using our approach. For more comprehensive cancer detection,

biomarkers beyond CD44 can be targeted. With the potential for multiplexing, the SERS-NP strategy can be applied for simultaneous detection of multiple biomarkers in one imaging session, which is a direction we will pursue.

Conclusions

A facile one-pot synthesis of SERS-NPs has been developed, which is applicable to a variety of Raman dyes including both resonant and non-resonant Raman dyes. Using the seed growth method assisted by tris base, the synthesized 50 nm spherical SERS-NPs have more homogeneous size and shape distribution, which is a significant improvement compared to those prepared with the more traditional direct sodium citrate assisted synthesis. Bright SERS Raman signals were observed with the NPs synthesized, which could be detected with fM sensitivity. The multiple flavors of the SERS-NPs available enabled multiplex imaging with the necessary algorithm established to unmix the flavors and accurately determine the ratios of various flavors present.

For biological detection, an important attribute of the SERS-NPs is their ability to selectively bind with the target of interests. The direct attachment of the targeting ligand HA to SERS-NPs gave relatively low binding to the target protein CD44. Instead, a new liposomal based synthesis strategy was established to install HA onto the SERS-NPs, which had significantly higher CD44 binding compared to the corresponding HA-SERS-NPs without the liposome formulation. The liposome-SERS-HA enabled successful image-guided removal of breast cancer via surgery from a spontaneous mouse breast cancer model. With their bright Raman signals, availability in multiple flavors, high biocompatibility and colloidal stabilities, and the high targeting abilities, the liposomal SERS particles prepared in this study have powerful translational potential for image guided surgery. Furthermore, the successful application of liposome-SERS-HA in real time imageguided surgery opens a new avenue to investigate polysaccharides as potential targeting agents for SERS applications complementing current antibody-based strategies.

Experimental section

Reagents

Sodium hyaluronan (10 kDa) was purchased from Lifecore Biomedicals. HS-PEG and HS-HA of different molecular weight were purchased from Creative PEGWorks. Trisodium citrate dihydrate (C₆H₅Na₃O₇·2H₂O, 99.0%), tris base (NH₂C(CH₂OH)₃, 99.9%), and gold(III) chloride trihydrate (HAuCl₄·3H₂O, 99.995%), 4,4'-dipyridyl (S420), d8-4,4'-dipyridyl (S421), trans-1,2-

bis(4-pyridyl)-ethylene (S440), 4-azobis(pyridine) (S481), 2,5-bis(4-pyridyl)-1,3,4-thiadiazole (\$493), IR780 and Cv5.5, cholesterol as well as other chemicals were purchased from Sigma Aldrich unless otherwise stated. 1,2-Dipalmitoyl-sn-glycero-3-PC (DPPC) was obtained from Cayman Chemical. Deionized water (Milli-Q grade, Millipore) with a resistivity of 18.2 M Ω cm was used throughout the experiment.

NP characterization

The size of the NPs was measured by dynamic light scattering (DLS) and surface charge was obtained by ζ potential using a Zetasizer Nano zs apparatus (Malvern, U.K.). SpectraMax M3 plate reader was used to record UV-vis absorption spectra. The TEM images of the NPs were acquired with a TEM (JEM- 2200FM) operating at 200 kV using Gatan multiscan CCD camera with Digital Micrograph imaging software.

Raman Measurements and Spectral Unmixing Processing.

Raman measurement was carried out using both Andor system (Figure S8) and Renishaw inVia Reflex Raman system. Principal component analysis (PCA) was employed for spectral unmixing to attain weight values.

Sodium citrate assisted synthesis of SERS NPs

A 250 mL Erlenmeyer flask was cleaned extensively by washing with Aqua regia, then with DI water. 100 mL MilliQ water was added to the 250 mL Erlenmeyer flask, boiled and discarded for further washing. Then MilliQ water (48 mL) and 25 mM HAuCl₄ solution (0.5 mL) were added into the 250 mL Erlenmeyer flask and capped with aluminum foil. For a standard hot plate (Corning PC-4200), the stirring was set to 500 RPM, and heating was set to 500 °C, for vigorous stirring and heating. Under vigorous stirring, the solution was heated to boiling, followed by the addition of sodium citrate (5 mg/mL, 0.75 mL). Color change occurred within 4 minutes, indicating the formation of Au-NPs. Subsequently, a solution of S440, S420, S421, or S481 (5 µL 1 mM) in DMF was added. Stirring was kept for another 2 minutes, followed by cooling down in ice bath, and centrifugation at 5000 g at 4 °C for 10 minutes to collect SERS NP pellet.

Tris base assisted synthesis of SERS NPs

Synthesis of 17 nm seeds: A 250 mL Erlenmeyer flask was cleaned extensively by washing with Aqua regia, then with DI water. MilliQ water (100 mL) was added to the 250 mL Erlenmeyer flask, boiled and discarded for further washing. MilliQ water (48 mL) was added into the Erlenmeyer flask and capped with aluminum foil. For a standard hot plate (Corning PC-4200),

5 439 6 460

8 461

9 10 462

467

474

479

480

485

468 22

469

45 481 46 402

30 473

the stirring was set to 500 RPM, and heating was set to 500 °C for vigorous stirring and heating. When the solution started to boil, HAuCl₄ solution (25 mM, 0.5 mL) was added, followed by the addition of 1% sodium citrate solution (1.5 mL). With the addition of sodium citrate, Au-NP formation was initiated. Color change occurred within 5 minutes, indicating the formation of Au-NPs. The solution was kept stirring for another 8 minutes after the addition of sodium citrate. Gold colloidal was then cooled down in an ice bath. The volume of the solution was adjusted to 50 mL.

Synthesis of 50 nm SERS NPs: A 250 mL Erlenmeyer flask was cleaned extensively by washing with Aqua regia, then with DI water. MilliQ water (100 mL) was added to the 250 mL Erlenmeyer flask, boiled and discarded for further washing. MilliQ water (91 mL) was added into 200mL Erlenmeyer flask and capped with aluminum foil. For a standard hot plate (Corning PC-4200), the stirring was set to 500 RPM, and heating was set to 500 °C for vigorous stirring and heating. When the solution started to boil, 0.1 M tris base (4 mL) was added. Then 3 mL seed solution was added, followed by the addition of 25 mM HAuCl₄ (1 mL). The addition of tetrachloroauric acid initiated the formation of AuNPs. Color change occurred within 3 minutes. Then 10 μL Raman dye solution (100 mM for S420, S421, S440, S481 and S493, 500 μM for IR780 and Cy5.5) was added and stirring was kept for exactly 1 minute. Then gold colloidal was cooled down in ice bath for 3 minutes, followed by centrifugation at 5000g at 4 °C for 10 minutes. Supernatant was carefully removed without disturbing the pellets. SERS NPs were redispersed into MilliQ water. Concentration was measured using calibration curve established with absorption at 527 nm.

Competitive ELISA

The competitive ELISA was performed using CD44-FC γ chimera (0.2 μ g/well, R&D systems, cat no. 3660-CD) as the coating antigen following a literature procedure. ^[57] The abilities of HA (10 kDa, 1 μ g/well, 100 μ L), or liposome-SERS-HA (at equivalent HA amount) to compete against b-HA (0.5 μ g/well, 100 μ L) for CD44 binding was determined.

MTS assay with SERS-NPs

4T1 cells (1 x 10⁵ cells/mL, 200 μL corresponding to 20,000 cells per well) were dispersed in RPMI cell culture media containing FBS (10 %) and cultured in a 96-well plate for 16 h in the presence of 5 % CO₂ at 37 °C. The media was removed, and the cells were washed two times with PBS. The cells were incubated with various concentrations (0 pM, 10 pM, 20 pM, 50 pM, 100 pM, 200 pM, 300 pM, and 500 pM) of liposome-SERS-PEG or liposome-SERS-HA for 4 h. The

supernatants were removed, and cells were washed with PBS two times. MTS reagent (Promega, cat no. G358C) dispersed in medium (17%) was added and incubated for another 3 h in the dark. A brown color appeared in the wells containing live cells. The absorption of each well was measured at 490 nm using a SpectraMax M3 plate reader, with the absorbance from wells without cells (blanks) subtracted as background from each sample.

Synthesis of liposome-SERS-HA/PEG

Liposome-SERS complexes were prepared through a modified thin film hydration method. Briefly, DPPC (2 mg) and cholesterol (0.5 mg) were dissolved in CHCl₃ / MeOH (v/v, 2:1, 0.5 mL), and dried using a rotary evaporator at 37 °C to form a lipid film. The film was hydrated with SERS-HA or SERS-PEG solution. For SERS-HA, SERS NP (200 pM, 500 µL) was mixed with 100 µL 10 mg/mL HS-HA (10 kDa) and incubated overnight. For SERS-PEG, SERS NPs (200 pM, 500 µL) were mixed with HS-PEG (5 kDa, 10 µL 10 mg/mL) and incubated overnight. During hydration, the solution was kept still for 30 minutes without sonication. Then the solution was pipetted up and down to facilitate the hydration process followed by water bath sonication. The complex was centrifuged down at 2500 g for 5 minutes, washed two times by repeated centrifugation to remove unbounded PEG, HA and empty liposome, and redispersed back into MilliQ water.

Stability of liposome-SERS-HA/PEG in PBS

Liposome-SERS-HA/PEG dissolved in water were placed in glass vials (1 mL, 200 pM). A phosphate-buffered saline (1x and 10x) solution (0.1 mL) was added to the vials. UV-vis measurement and dynamic light scattering (DLS) measurement were carried out before and after the addition of PBS solution.

Stability of liposome-SERS-HA/PEG in serum

An aqueous solution of liposome-SERS-HA/PEG in water was introduced to undiluted mouse serum in a 1 : 1 v/v ratio, followed by a 24-hour incubation at 37 °C. Afterward, the samples were centrifuged at 10,000 rpm, and the supernatants were removed. The samples were then resuspended in distilled water and centrifuged again at 10,000 rpm. The precipitates were collected and re-suspended, and UV-vis and DLS measurements were conducted.

Carbazole assay for hyaluronan quantification

The sample (50 μL) was mixed with sodium tetraborate in sulfuric acid (25 mM, 200 μL) in a 0.7 mL tube, and heated at 100 °C for 10 minutes. This was followed by the addition of 0.125%

⁴ 521

5 6 522

523

524

541

542

547

548

529 20

530 22 **531**

30 535

536 537

carbazole in absolute ethanol (50 μ L) after the sulfuric acid solution cooled down. The mixture was then heated at 100 °C for another 10 minutes. After cooling down to room temperature, the mixture (200 μ L) was transferred into wells in a 96 well microtiter plate, and the optical densities at 550 nm were measured.

Cell culture for Raman imaging

Breast cancer cell line, 4T1cells (~0.2 x 10⁶ cells/mL) were grown on custom-made (6 mm x 6 mm x 1 mm thick, CHEMGLASS Microscope Slide, GRAINGER) quartz-bottomed 100 mm Petri dish containing 13 mL RPMI 1640 culture medium supplemented with 10% v/v FBS and 1% penicillin-streptomycin in an incubator at 37 °C with 5% CO₂ for 2 days. Cells grown on quartz were transferred into 48 well-plate and fixed with 10% NBF solution upon the incubation for 30 minutes at 4 °C following washing with PBS for two times. The cells were incubated with liposome-SERS-HA/PEG (100 pM) for 3 hours at 4 °C with a gentle shaking of 90 rpm following two times washing by PBS.

Image-guide surgery through SERS imaging

The staining solution was prepared by mixing Liposome-S421 SERS-HA (500 pM) and Liposome-S440 SERS-PEG (500 pM) at 1 : 1 ratio. MMTV-PyMT transgenic mice were purchased from the Jackson Laboratory. In a span of 4 months, the female mice showed the spontaneous onset of palpable breast cancer. The mice were housed at Michigan State University's Laboratory Animal Resources Facility. All activities and protocols related to the animal study received approval from the Institutional Animal Care and Used Committee (IACUC) at Michigan State University. An MMTV mouse was put under anesthesia with 5% isoflurane in oxygen. The tumor area was first opened, and the tissue background was scanned. Then 50 µL of the staining solution was topically applied to both the tumor area and surrounding normal area. After 15 minutes, the staining area was washed with PBS three times. Raman mapping of the tissue area was obtained before and after the washing process. Then a portion of the tumor was removed, followed by repeated staining and imaging. The whole process is repeated until all the tumor is removed. Dissected tissue was fixed with paraformaldehyde (4 %) for H&E and IHC staining. All animal experiments were performed in accordance with the guidelines of the Institutional Animal Care and Use Committee (IACUC) of Michigan State University (approved protocol #: PROTO202100095).

1 2	
3 4 5	552
6	553
7 8	554
9	555
11	556
13	557
14 15	558
16 17	559
18 19	560
20	561
22	562
23 24	563
25 26	564
27 28	565
29	566
30 31	567
32 33	568
2⊿	569
35 36	
37	570
38 39	571
40	572
41 42	312
43 44	573
45	574
46 47	J/4
48	575
49 50	576
51	- , 5

Statistical Analysis

- 554 All data were represented as mean ± standard deviation (SD) (n=3) unless specified otherwise.
- 555 Statistical significance between two groups was assessed using two-way ANOVA and the
- 556 significance level was set at a value of 0.05. The data were indicated as ns: P > 0.05; *: P < 0.05.
- 557 The statistical analysis was performed using GraphPad.

559 **Ethics Statement**

560 All animal experiments were performed in accordance with the guidelines of the 561 Institutional Animal Care and Use Committee (IACUC) of Michigan State University (approved

562 protocol #: PROTO202100095).

Acknowledgments and funding statement:

- 565 We are grateful for the financial support from the National Institute of General Medical Sciences,
- 566 NIH (R01GM072667), the National Science Foundation (grant numbers 1808436, 1918074, and
- 567 2237142-CAREER) and Michigan State University.

Conflict of interest disclosure

570 The authors declare no competing interests.

Data availability statement

- 573 The Supporting Information is available free of charge at ####.
- 574 Supplementary figures S1-S9, table S1.

575

576 **References:**

52 577

- 578 [1] R. Pilot, R. Signorini, C. Durante, L. Orian, M. Bhamidipati, L. Fabris, *Biosensors* 2019, 9, 57. 55 579
- 56 580 B. Sharma, R. R. Frontiera, A.-I. Henry, E. Ringe, R. P. Van Duyne, *Mater. Today* 2012, [2]
- 57 581 *15*, 16.
- 58 Z. Du, Y. Qi, J. He, D. Zhong, M. Zhou, Wiley Interdiscip. Rev. Nanomed. 582
- 59 60 583 Nanobiotechnology 2021, 13, e1672.

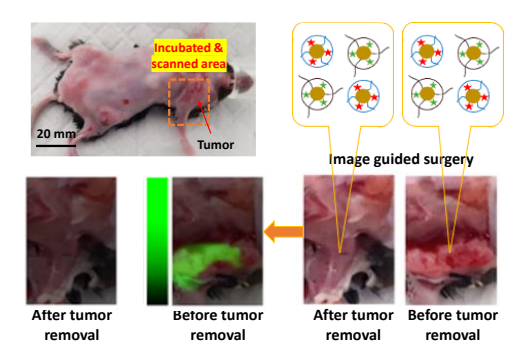
- 1 2 3 4
- 584 X. M. Qian, S. M. Nie, Chem. Soc. Rev. 2008, 37, 912. [4]
- 5 585 S. Zeng, K.-T. Yong, I. Roy, X.-Q. Dinh, X. Yu, F. Luan, *Plasmonics* **2011**, *6*, 491. [5] 6
- J. Polte, T. T. Ahner, F. Delissen, S. Sokolov, F. Emmerling, A. F. Thünemann, R. 586 [6] 7
- 587 Kraehnert, J. Am. Chem. Soc. 2010, 132, 1296. 8
- 9 588 Y. Wang, B. Yan, L. Chen, Chem. Rev. 2013, 113, 1391. [7]
- 10 589 Á. I. López-Lorente, Anal. Chim. Acta 2021, 1168, 338474. [8]
- 11 N. D. Israelsen, C. Hanson, E. Vargis, Sci. World J. 2015, 2015, 124582 and references 590 [9] 12 cited therein. 13 591
- 14 592 S. Hong, X. Li, J. Nanomater. **2013**, 2013, 790323. [10]
- ¹⁵ 593 F. Meikun, F. S. A. Gustavo, G. B. Alexandre, Anal. Chim. Acta 2020, 1097, 1. [11]
- 16 594 [12] S. E. J. Bell, G. Charron, E. Cortés, J. Kneipp, M. L. de la Chapelle, J. Langer, M. 17
- 18 595 Procházka, V. Tran, S. Schlücker, Angew. Chem. Int. Ed. 2020, 59, 5454.
- 19 596 L. A. Lane, X. Qian, S. Nie, Chem. Rev. 2015, 115, 10489.
- 20 597 Y. Wang, S. Kang, A. Khan, G. Ruttner, S. Y. Leigh, M. Murray, S. Abeytunge, G. [14]
- ²¹ 598 Peterson, M. Rajadhyaksha, S. Dintzis, S. Javid, J. T. C. Liu, Sci. Rep. 2016, 6, 21242. 22
- 599 M. Arruebo, M. Valladares, Á. González-Fernández, J. Nanomater. 2009, 2009, 439389. [15] 23
- 24 600 [16] S. Okyem, O. Awotunde, T. Ogunlusi, M. B. Riley, J. D. Driskell, *Langmuir* 2021, 37, 2993. 25 601
- 26 602 O. E. Eremina, A. T. Czaja, A. Fernando, A. Aron, D. B. Eremin, C. Zavaleta, ACS Nano $\lceil 17 \rceil$ 27
- 603 **2022**, 16, 10341. 28
- 29 604 S. Harmsen, M. A. Wall, R. Huang, M. F. Kircher, *Nature Protoc.* 2017, 12, 1400. [18]
- [19] B. Mir-Simon, I. Reche-Perez, L. Guerrini, N. Pazos-Perez, R. A. Alvarez-Puebla, Chem. 30 605
- 31 606 Mater. 2015, 27, 950.
- 32 607 T. Nagy-Simon, M. Potara, A.-M. Craciun, E. Licarete, S. Astilean, J. Colloid Interface [20] 33
- 608 Sci. 2018, 517, 239. 34
- 35 609 H. Xia, S. Bai, J. r. Hartmann, D. Wang, *Langmuir* **2010**, *26*, 3585. [21]
- J. Dong, P. L. Carpinone, G. Pyrgiotakis, P. Demokritou, B. M. Moudgil, KONA Powder 36 610 [22]
- ³⁷ 611 Part. J. 2020, 37, 224.
- 38 612 P. Zhang, C. Xi, C. Feng, H. Xia, D. Wang, X. Tao, CrystEngComm 2014, 16, 5268. [23] 39
- 40 613 C. Ziegler, A. Eychmuller, *J. Phys. Chem. C* **2011**, *115*, 4502. [24]
- 41 614 N. G. Bastús, J. Comenge, V. Puntes, *Langmuir* **2011**, *27*, 11098. [25]
- 42 615 P. Zhang, Y. Li, D. Wang, H. Xia, Part. Part. Syst. Charact. 2016, 33, 924. [26]
- ⁴³ 616 [27] Y. Li, P. Zhang, J. Duan, S. Ai, H. Li, CrystEngComm 2017, 19, 318.
- 44 617 [28] B. Baruah, C. Craighead, C. Abolarin, Langmuir 2012, 28, 15168. 45
- Y. Huang, D.-H. Kim, *Langmuir* **2011**, *27*, 13861. 46 618 [29]
- 47 619 [30] N. R. Jana, T. Pal, Adv. Mater. 2007, 19, 1761.
- 48 620 [31] X. Lu, A. Dandapat, Y. Huang, L. Zhang, Y. Rong, L. Dai, Y. Sasson, J. Zhang, T. Chen, 49
- 621 RSC Adv. 2016, 6, 60916. 50

- 622 [32] X. Huang, M. A. El-Sayed, J. Adv. Res. 2010, 1, 13. 51
- [33] C. L. Zavaleta, B. R. Smith, I. Walton, W. Doering, G. Davis, B. Shojaei, M. J. Natan, S. 52 623
- S. Gambhir, Proc. Natl. Acad. Sci. U.S.A. 2009, 106, 13511. 53 624
- 54 625 [34] A. J. Day, G. D. Prestwich, J. Biol. Chem. 2002, 277, 4585. 55
- 626 [35] J. Lesley, J. Biol. Chem. 2000, 275, 26967–26975. 56
- R. Tsuji, S. Ogata, S. Mochizuki, Bioorg. Chem. 2022, 121, 105666. ₅₇ 627 [36]
- 58 628 [37] A. Maiti, G. Maki, P. Johnson, Science 1998, 282, 941.
- 59 629 D. Naor, R. V. Sionov, D. Ish-Shalom, Adv. Cancer Res. 1997, 71, 241. [38] 60

- 1 2 3
- 630 [39] L. T. Senbanjo, M. A. Chellaiah, Front. Cell Dev. Biol., 2017, 5.
- 6 631 [40] S. Misra, P. Heldin, V. C. Hascall, N. K. Karamano, S. S. Skandalis, R. R. Markwald, S.
- ⁷ 632 Ghatak, *FASEB J.* **2011**, *278*, 1429.
- 8 633 [41] B. P. Toole, T. N. Wight, M. I. Tammi, J. Biol. Chem. 2002, 277, 4593.
- ⁹ 634 [42] H. Ponta, L. Sherman, P. A. Herrlich, *Nat. Rev. Mol. Cell Biol.* **2003**, *4*, 33.
- 10 635 [43] M. Li, J. Sun, W. Zhang, Y. Zhao, S. Zhang, S. Zhang, Carbohydrate Polym. 2021, 251,
- 12 636 117103.
- 13 637 [44] K. Liu, X. Huang, Carbohydr. Res. 2022, 511, 108500.
- 14 638 [45] S. H. Nasr, Z. Rashidijahanabad, S. Ramadan, N. Kauffman, N. Parameswaran, K. R. Zinn,
- ¹⁵ 639 C. Qian, R. Arora, D. Agnew, X. Huang, *Nanoscale* **2020**, *12*, 9541.
- 16 640 [46] S. H. Nasr, A. Tonson, M. H. El-Dakdouki, D. C. Zhu, D. Agnew, R. Wiseman, C. Qian,
- 18 641 X. Huang, ACS Appl. Mater. Interfaces **2018**, 10, 11495.
- 19 642 [47] W. Wang, D. Li, Y. Zhang, W. Zhang, P. Ma, X. Wang, D. Song, Y. Sun, Microchimica
- ²⁰ 643 *Acta* **2020**, *187*, 604.
- 21 644 [48] J. L. Montaño-Priede, J. P. Coelho, A. Guerrero-Martínez, O. Peña-Rodríguez, U. Pal, J.
- ²² 645 *Phys. Chem. C* **2017**, *121*, 9543.
- 24 646 [49] Y. Zhang, X. Li, B. Xue, X. Kong, X. Liu, L. Tu, Y. Chang, Sci. Rep. 2015, 5, 14934.
- 25 647 [50] C.-C. Huang, C.-H. Huang, I. T. Kuo, L.-K. Chau, T.-S. Yang, Colloids Surf. A
- ²⁶ 648 *Physicochem. Eng. Asp.* **2012**, 409, 61.
- ²⁷ 649 [51] Y. Xue, X. Li, H. Li, W. Zhang, *Nat. Commun.* **2014**, *5*, 1.
- ⁻⁻₂₉ 650 [52] M.-Y. Lee, J.-A. Yang, H. S. Jung, S. Beack, J. E. Choi, W. Hur, H. Koo, K. Kim, S. K.
- 30 651 Yoon, S. K. Hahn, ACS Nano 2012, 6, 9522.
- 31 652 [53] O. Gotov, G. Battogtokh, D. Shin, Y. T. Ko, Journal of industrial and engineering
- 32 653 *chemistry* **2018**, *65*, 236.
- 33 654 [54] H. Lee, K. Lee, I. K. Kim, T. G. Park, *Biomaterials* **2008**, *29*, 4709.
- 35 655 [55] X. Li, H. Zhou, L. Yang, G. Du, A. S. Pai-Panandiker, X. Huang, B. Yan, Biomaterials
- **2011**, *32*, 2540.
- ³⁷ 657 [56] X. Lu, X. Huang, *Glycoconjugate J.* **2015**, *32*, 549.
- 38 658 [57] M. Kamat, K. El-Boubbou, D. C. Zhu, T. Lansdell, X. Lu, W. Li, X. Huang, *Bioconjugate*
- 39 659 *Chem.* **2010**, 21, 2128.
- 41 660 [58] Y. Xia, C. Xu, X. Zhang, P. Ning, Z. Wang, J. Tian, X. Chen, Nanoscale 2019, 11, 5822.
- 42 661 [59] A. Dėdinaitė, D. C. F. Wieland, P. Bełdowski, P. M. Claesson, Adv. Colloid Interface Sci.
- ⁴³ 662 **2019**, *274*, 102050.
- 44 663 [60] A. Ewurum, A. A. Alur, M. Glenn, A. Schnepf, D. Borchman, *BMC Chem.* **2021**, *15*, 36.
- 46 664 [61] M. Cesaretti, E. Luppi, F. Maccari, N. Volpi, Carbohydrate Polym. 2003, 54, 59.
- 47 665 [62] A. Ewurum, A. A. Alur, M. Glenn, A. Schnepf, D. Borchman, *BMC Chem.* **2021**, *15*, 1.
- 48 666 [63] K. Liu, W. M. McCue, C.-W. Yang, B. C. Finzel, X. Huang, *Carbohydr. Polym.* **2023**, *300*, 49 667 120255
- ⁴⁹ 50 667 120255.

- 668 [64] X. Yang, S. K. Sarvestani, S. Moeinzadeh, X. He, E. Jabbari, *PLoS One* **2013**, *8*, e59147.
- 52 669 [65] K. L. Kummerow, L. Du, D. F. Penson, Y. Shyu, M. A. Hooks, *JAMA Surg.* **2015**, *150*, 9.
- 53 670 [66] M. T. Garcia, B. S. Mota, N. Cardoso, A. L. C. Martimbianco, M. D. Ricci, F. M. Carvalho,
- ⁵⁴ 671 R. Gonçalves, J. M. Soares Junior, J. R. Filassi, *PLOS ONE* **2021**, *16*, e0248768.
- 55 672 [67] Consensus Guideline on Breast Cancer Lumpectomy Margins,
- https://www.breastsurgeons.org/docs/statements/Consensus-Guideline-on-Breast-Cancer-
- Lumpectomy-Margins.pdf, accessed: March 15th, 2023.

- L. E. McCahill, R. M. Single, E. J. Aiello Bowles, H. S. Feigelson, T. A. James, T. Barney, J. M. Engel, A. A. Onitilo, *JAMA* **2012**, *307*, 467.
 - Y. W. Wang, N. P. Reder, S. Kang, A. K. Glaser, Q. Yang, M. A. Wall, S. H. Javid, S. M.
- Dintzis, J. T. C. Liu, Cancer Res. 2017, 77, 4506.
- Y. W. Wang, Q. Yang, S. Kang, M. A. Wall, J. T. C. Liu, J. Biomed. Opt. 2018, 23, 1.
- [71] E. Y. Lin, J. G. Jones, P. Li, L. Zhu, K. D. Whitney, W. J. Muller, J. W. Pollard, Am. J. Pathol. 2003, 163, 2113.
- 13 682 [72] J. E. Maglione, D. Moghanaki, L. J. T. Young, C. K. Manner, L. G. Ellies, S. O. Joseph,
- B. Nicholson, R. D. Cardiff, C. L. MacLeod, Cancer Res. 2001, 61, 8298.
- N. Al-Othman, A. Alhendi, M. Ihbaisha, M. Barahmeh, M. Alqaraleh, B. Z. Al-Momany, Breast Dis. 2020, 39, 1.
- 18 686



695

690

22 692 23 693

694

Table of Content text:

A method has been established to produce colloidally stable and bright SERS-nanoparticles (SERS-NPs) with uniform core sizes. Furthermore, a new liposome-based approach has been developed to install a targeting carbohydrate ligand, i.e., hyaluronan, onto the SERS-NPs bestowing significantly enhanced binding affinity to its biological receptor CD44 overexpressed on tumor cell surface, enabling image-guided surgery to completely remove breast cancer.

Supporting Information

Click here to access/download

Supporting Information

Liposome SERS HA Revised SI clean copy.docx

Production Data

Click here to access/download

Production Data

Liposome SERS HA Revised Final Clean Copy.docx

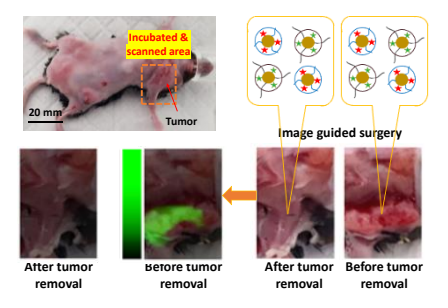


Table of Content text:

A method has been established to produce colloidally stable and bright SERS-nanoparticles (SERS-NPs) with uniform core sizes. Furthermore, a new liposome-based approach has been developed to install a targeting carbohydrate ligand, i.e., hyaluronan, onto the SERS-NPs bestowing significantly enhanced binding affinity to its biological receptor CD44 overexpressed on tumor cell surface, enabling image-guided surgery to completely remove breast cancer.